Title
COLLISIONAL EXCITATION AND LORENTZ IONIZAITON OF 10-MeV HYDROGEN ATOMS

Author
Berkner, Klaus H.

Publication Date
1964-03-13

UCRL-11249 errata

University of California

Ernest O. Lawrence Radiation Laboratory

COLLISIONAL EXCITATION AND LORENTZ IONIZATION OF 10-MeV HYDROGEN ATOMS

Berkeley, California

DISCLAIMER

UNIVERSITY OF CALIFORNIA

Lawrence Radiation Laboratory
Berkeley, California

July 23, 1964

ERRATA

TO: All recipients of UCRL-11249

FROM: Technical Information Division

Subject: UCRL-11249 "COLLISIONAL EXCITATION AND LORENTZ IONIZATION OF 10-MeV HYDROGEN ATOMS" by Klaus H. Berkner (Ph. D. Thesis), March 13, 1964

Please make the following corrections on subject report.

Page 10, Fig. 3, second column of Legend on drawing reads: AA 301
It should read: AA 501

Page 18, Table II, first column third line reads: 3s - 3d
It should read: 2s - 3d

Page 54, Table VI, heading of 6th column reads: $\frac{n\text{th level}}{(n+1)\text{th level}}$
It should read: $\frac{n\text{th level}}{(n+1)\text{th level}}$;

Table VI, heading of 7th column reads: $\frac{n\text{th level}}{(n+1)\text{th level}}$
It should read: $\left(\frac{n+1}{n}\right)^3$

Page 55, last equation reads: 1.9×10^{-18}
It should read: $\frac{1.9}{n^3}\times10^{-18}$

Page 60, Fig. 23 caption, add to caption:
The point is the experimental result for $N_8 + N_9$.

Page 90, Ref. 49 reads: ··· submitted for publication in Phys. Rev., 1964
It should read: ··· Phys. Rev. 134, A1461 (1964)

UCRL-11249

UNIVERSITY OF CALIFORNIA

Lawrence Radiation Laboratory
Berkeley, California

AEC Contract No. W-7405-eng-48

COLLISIONAL EXCITATION AND LORENTZ IONIZATION OF 10-MeV HYDROGEN ATOMS

Klaus H. Berkner

(Ph. D. Thesis)

March 13, 1964

Printed in USA. Price $2.00. Available from the
Office of Technical Services
U. S. Department of Commerce
Washington 25, D.C.

Contents

COLLISIONAL EXCITATION AND LORENTZ IONIZATION OF 10-MeV HYDROGEN ATOMS

Klaus H. Berkner

Lawrence Radiation Laboratory
University of California
Berkeley, California

March 13, 1964

ABSTRACT

Ten-MeV hydrogen atoms with a population distribution covering all excited states are produced by collisional dissociation of 20-MeV H_2^+ ions. The populations of the higher excited levels are removed by Lorentz ionization, and the levels are then repopulated by collisional excitation of the atoms in molecular or weakly ionized hydrogen targets. The populations of the levels n = 6 to 9 are determined by a second Lorentz ionization.

The threshold fields for Lorentz ionization of the levels n = 5 to 9 are found to be in good agreement with theoretical calculations for electric-field ionization. The populations of the levels n = 6 to 9 of atomic hydrogen produced by collisional dissociation of H_2^+ on H_2 are found to be $N_n/N_1 \approx 3/n^3$, a distribution that is consistent with theoretical estimates.

For hydrogen plasma targets, excitation cross sections have been measured for collisions with electrons and ions. Cross sections for transitions from the levels n =5, 6 to the levels n' = 6, 7, 8, 9 and upper limits for the transitions n = 1 or 4 to n' = 6 or 7 have been obtained. These are compared with calculations in the first Born, Bethe, and impact-parameter approximations; good agreement is found for all transitions, although those with $\Delta n = 2$ are somewhat larger than calculated.

For molecular-hydrogen targets, cross sections are obtained for excitation from all levels $n \leq 4, 5, 6$ to the levels $n' = 6, 7, 8,$ and 9. Cross sections for the individual transitions from $n = 1, 4, 5, 6$ to the levels $n' = 6, 7, 8, 9$ have been deduced from these results. These cross sections differ markedly from those for charged-particle collisions: They are smaller by at least two orders of magnitude; they increase slowly with n; and $\Delta n > 1$ transition probabilities are of the same order of magnitude as $\Delta n = 1$ transitions, so that only upper limits for the cross sections of individual transitions could be obtained. These observations are consistent with extrapolations of first Born approximation calculations for lower n values.

I. INTRODUCTION

A. Background and Statement of Problem

A hydrogen atom placed in an external electric field will ionize when the force exerted by this field on the proton-electron system becomes comparable to the mutual Coulomb attraction of the system. When the external field is the equivalent $\underset{\sim}{v} \times \underset{\sim}{B}$ electric field seen in the rest frame of an atom moving with velocity $\underset{\sim}{v}$ through a magnetic field $\underset{\sim}{B}$, this process is called Lorentz ionization. The ionization rate of a particular excited level is determined by the energy of that level and the strength of the external field; the more highly excited levels require weaker electric fields for ionization than the more tightly bound levels. It is therefore possible to determine the population of the excited levels of hydrogen by Lorentz ionization. In this experiment we develop this technique and use it to determine the population of the quantum levels n = 6 to 9 of atomic hydrogen. We then study the changes in these populations due to non-ionizing collisions with hydrogen molecules and with protons and electrons in a weakly ionized plasma.

The probability of ionization for a ground-state hydrogen atom in an external electric field was first calculated by Oppenheimer in 1928.[1] He concluded that ionization became appreciable at field strengths about one-tenth as large as those required to make the classical Bohr orbit unstable. Shortly thereafter strong-field ionization was observed by Traubenberg and co-workers.[2,3] During a spectroscopic investigation of the Stark effect for the Balmer series, they observed that the red Stark component of $H\zeta$ (arising from the most tightly bound Stark state) disappeared at 120 kV/cm, whereas the blue component (arising from the least tightly bound Stark state) disappeared at 180 kV/cm. This same trend was observed for the lower terms of the Balmer series down to $H\gamma$, which disappeared between 700 and 1000 kV/cm. These results were

successfully explained by Lanczos, who considered the change in the atom's electronic potential caused by the external field and used a one-dimensional WKB approximation to calculate the barrier-penetration probability for the levels n = 5 to 8.[4,5] A spectral line disappears when a bound electron can tunnel through the potential barrier in a time that is shorter than its radiative lifetime. A three-dimensional WKB calculation has recently been carried out by Rice and Good for the two extremes (the components of the Balmer series nearest the red and nearest the blue) of the Stark states for n = 5 to 7.[6] These calculations show that the blue components have a longer lifetime against strong-field ionization than predicted by Lanczos. Bailey and Hiskes have extended these calculations for all Stark states for the levels n = 1 to 7 and for the extreme Stark states up to n = 25.[7]

Recently experiments on electric-field[8,9] and Lorentz[9-11] ionization have been conducted with energetic beams of hydrogen atoms. In these experiments the resulting protons were detected as a function of the field strength. The results indicate that this technique can be used to determine the population of a quantum level n, although some ambiguity results for $n \geq 7$ due to the overlapping of the states of various levels.

Work on inelastic collisions of hydrogen atoms with electrons, protons, or other hydrogen atoms has been reviewed in the literature,[12-18] and a brief survey of the available results is given in Appendix A. We thus limit ourselves here to a few general remarks about excitation cross sections and refer the reader to Appendix A for the details.

Experimental cross sections for excitation by electron impact have been reported only for ground-state hydrogen atoms. These results agree with theoretical calculations in the first Born approximation (FBA) for electron energies > 200 eV; at lower energies, however, the FBA predictions are typically twice as large as the experimental results. More elaborate theoretical models have been used, but none of the results agree with the experimental results at low energies.

Recently FBA calculations for excitation by electron impact of excited hydrogen atoms have been carried out by Milford and coworkers,[19-24] but no experiments have yet been reported for such collisions.

For H-H collisions, excitation cross sections have been calculated in the FBA for some of the lower excited levels ($n \leq 4$).[16, 25] The only experimental cross sections that have been reported are the early results of the present experiment for the $n = 6$ to 7 transition induced by collisions with H_2.[11]

The scarcity of experimental results on collisional excitation is due, in large part, to the difficulty of observing the population of excited states. The spectroscopic means for determining the populations can now be supplemented by Lorentz ionization, although the resolution of the individual states within a level is lost in the process. Furthermore, the use of Lorentz ionization in the formation of energetic plasmas has aroused new interest in excitation cross sections.

One of the techniques under investigation for creating an energetic plasma within a closed-magnetic-field geometry is neutral injection. A beam of energetic (20 keV or higher) hydrogen or deuterium atoms is ionized in the confinement region, and the resulting charged particles are trapped by the magnetic field. The ionization results partly from collisions with neutrals, protons, and electrons already present in the confinement region and partly from the Lorentz force.[8, 26, 27] In a typical neutral-injection experiment, the Lorentz field is sufficient to ionize only excited hydrogen atoms in the quantum levels $n \geq 10$. Although fewer than 0.1% of the incident atoms are in these levels (see Sec. V. B.), their contribution can appreciably enhance the growth rate of the ion density.[8, 27] As the plasma builds up, successive collisions with the plasma will excite some of the more tightly bound levels to levels than can be Lorentz ionized. Hiskes has estimated that this inverted cascade can increase the final ion

density by at least two orders of magnitude in the present experiments.[28,29] His estimates are based on excitation cross sections calculated by Milford and co-workers.[21-23] These calculations are verified in the present experiment.

In this experiment we determine by Lorentz ionization the populations of the quantum levels n = 6 to 9 of a beam of 10-MeV hydrogen atoms. At this high energy we can obtain high Lorentz fields (43.7 kV/cm per kG) with dc magnets, and we can neglect charge exchange of protons formed by Lorentz ionization. This high energy also puts us in the region of validity of the FBA. Changes in the populations of these levels due to collisions in molecular and weakly ionized hydrogen targets are studied to determine absolute values for the cross sections for collisional excitation of these levels. These cross sections are averages over the states of a given level n. The results are compared with Born-approximation calculations.

B. List of Symbols

a.u.	Atomic units.
B	Magnetic field.
E	Kinetic energy.
F	Electric field.
FBA	First Born approximation.
Hα ··· Hζ	Terms in the Balmer series.
H(n, ℓ)	An excited hydrogen atom with principal quantum number n and orbital quantum number ℓ.
K	Change of momentum of projectile caused by collision.
level	All quantum states of an atom described by the principal quantum number n.
m_ℓ	Orbital magnetic quantum number.
m_s	Spin magnetic quantum number.
n^*	The highest level of the incident H^0 beam that is populated.

n_1, n_2	Parabolic quantum numbers corresponding to coordinates $\zeta = r + z$ and $\eta = r - z$.
N_n	Number of particles in the level n.
$\underset{\sim}{v}$	Velocity of neutral atom in the laboratory frame.
v_p	Relative velocity of projectile with respect to target atom before the collision.
v_q	Relative velocity of projectile with respect to target atom after the collision.
a	1/137. Fine-structure constant.
π	3.30×10^{13} p (microns) ℓ (cm). Number of target particles per cm^2 traversed by the beam; i. e. target thickness.
$\Pi = NL$	Total target thickness
πa_0^2	0.88×10^{-16} cm^2. Atomic unit for cross sections (area of first Bohr orbit).
$\sigma_{C,n}$	Cross section for electron capture by a proton to form an atom in the level n.
$\sigma_{n,C}$	Cross section for ionization of level n.
$\sigma_{n,m}$	Cross section for collisional excitation from the level n to the level m.
μ_0	Bohr magneton.

II. RÉSUMÉ OF PERTINENT THEORETICAL CALCULATIONS

A. Lorentz Ionization of the Hydrogen Atom

Theoretical calculations have been reported for ionization of hydrogen atoms in strong electric field, but not for Lorentz ionization. We assume that the electric-field calculations also apply to the Lorentz ionization of 10-MeV hydrogen atoms. The justification for this assumption is given in Appendix B.

An electric field distorts the electronic potential of an atom from a potential well to a barrier of finite width. This distortion causes the well-known Stark shift of the energy levels.[30] It also creates a finite probability for ionization by barrier penetration.[1-7,26,30] As the height and width of the barrier decrease with increasing field strength, successively lower bound states are completely destroyed. This process is qualitatively illustrated in Fig. 1.

A quantitative description requires the solution of the Schroedinger equation for an atom in an electric field. This equation is separable in parabolic coordinates, but the separated equations cannot be solved exactly. Approximate solutions for the energy levels have been obtained by perturbation theory[30] and in the WKB approximation.[5,6,30] The resulting WKB wave functions have been used to determine the barrier-penetration probability.[5-7,30,31] Of the various methods used, that of Rice and Good is the most rigorous.[6,7] Assuming that the electron is bound at $t = 0$, they build up wave functions from the three-dimensional WKB solutions to describe this initial state and calculate the outward probability current that develops in time.

The results of Bailey and Hiskes[7] (using the Rice and Good[6] model) for the extreme Stark components of the levels $n = 5$ to 9 are shown in Fig. 2. Ionization of a particular level n will occur over the field range indicated due to a population distribution over all Stark states within a given level. Note that for $n \geq 7$ the threshold

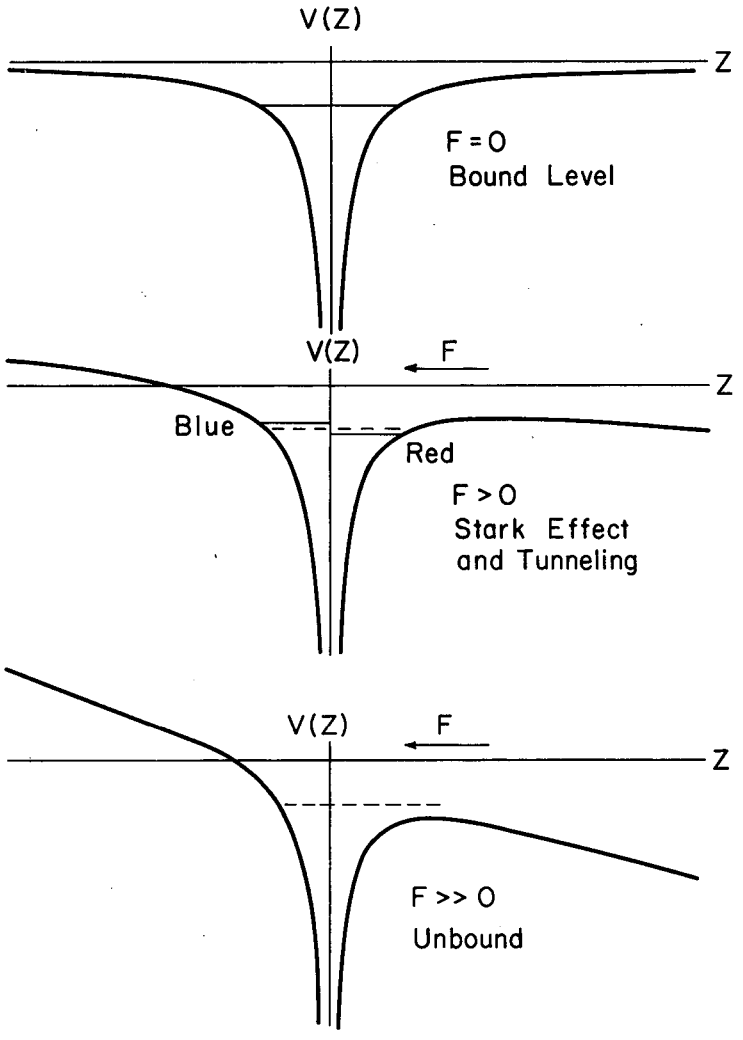

Fig. 1. Distortion of the electronic potential of a hydrogen atom caused by an electric field F.

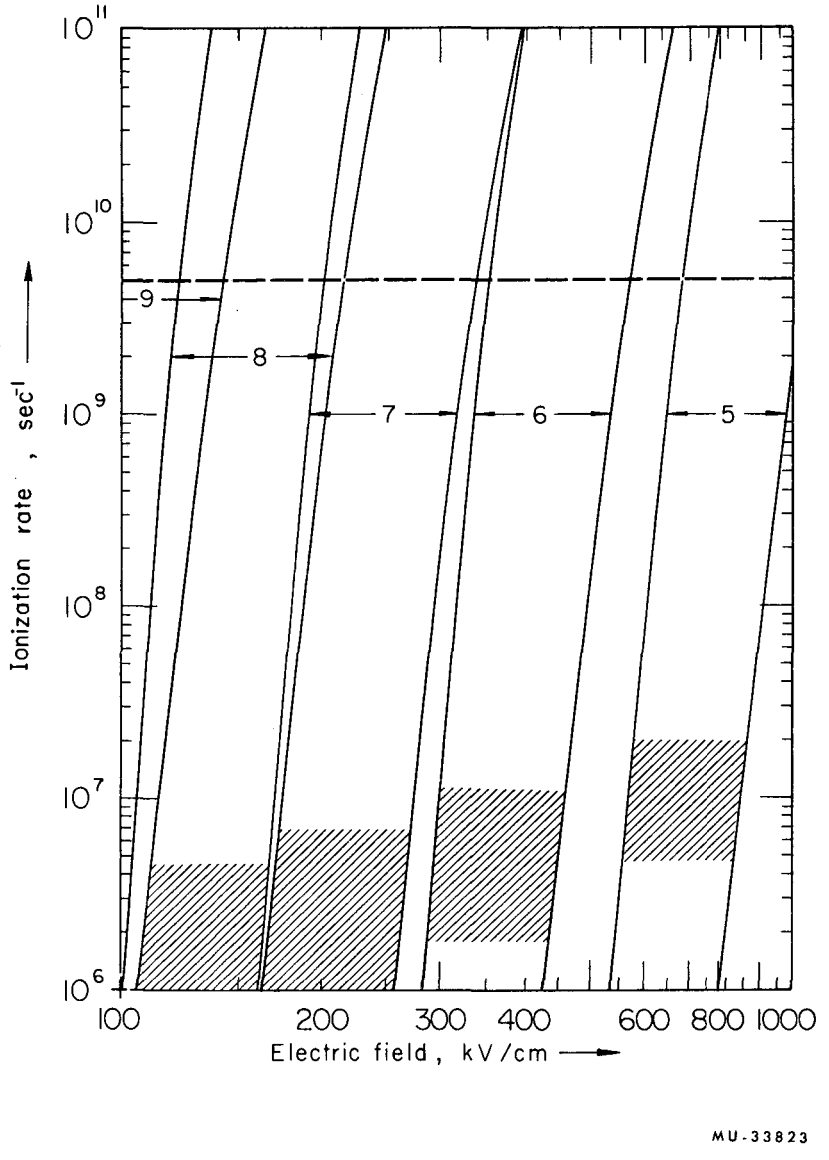

Fig. 2. Ionization rate vs field strength for the extreme Stark components of the n = 5 to 9 levels, using the Rice and Good model (from Ref. 7). The shaded region indicates the range of rates for spontaneous radiative transitions to lower levels for the various Stark states of each level. The dashed line is the reciprocal of the mean lifetime in the field profile used in this experiment (see Sec. III. C. 1). To achieve this ionization rate for the n = 4 level, 1300 to 1600 kV/cm are required.

fields for states of neighboring levels begin to overlap. This becomes more pronounced for very large n, and the thresholds for states of as many as five different levels may overlap for n = 25. Various states (n_1, n_2, m) of each level have different lifetimes for radiative decay to lower states, and the shaded regions indicate the range of spontaneous radiative transition rates for the states of each level.[32]

When the ionization rate for a particular state is much larger than the rate of radiative decay, that state will be depopulated by field ionization. In such a case, the population of a level n can be determined experimentally by measuring the number of ions that are produced as the electric-field strength is increased over the range that will ionize all the states of that level. This method should provide unambiguous results for n = 5 and 6; for n = 7, 8, and 9 some uncertainty in the measurement of the population will arise because of the overlapping of some of the states within these levels.

The probability of ionization for all Stark states of the level n = 7 is shown in Fig. 3.[7] This illustrates the almost uniform spacing of states in the lower 80% of the range of the electric field for ionization of this level. Only a small fraction of the Stark states are in the upper 20% of the electric-field range. The same conclusion can be reached from similar plots for the other levels. Thus, if the states of a given level are statistically populated, the small overlap between n = 7, 8, and 9 shown in Fig. 2 will not seriously affect the determination of the population of these levels, since only a small fraction of the population of the higher level will ionize in the overlap region.

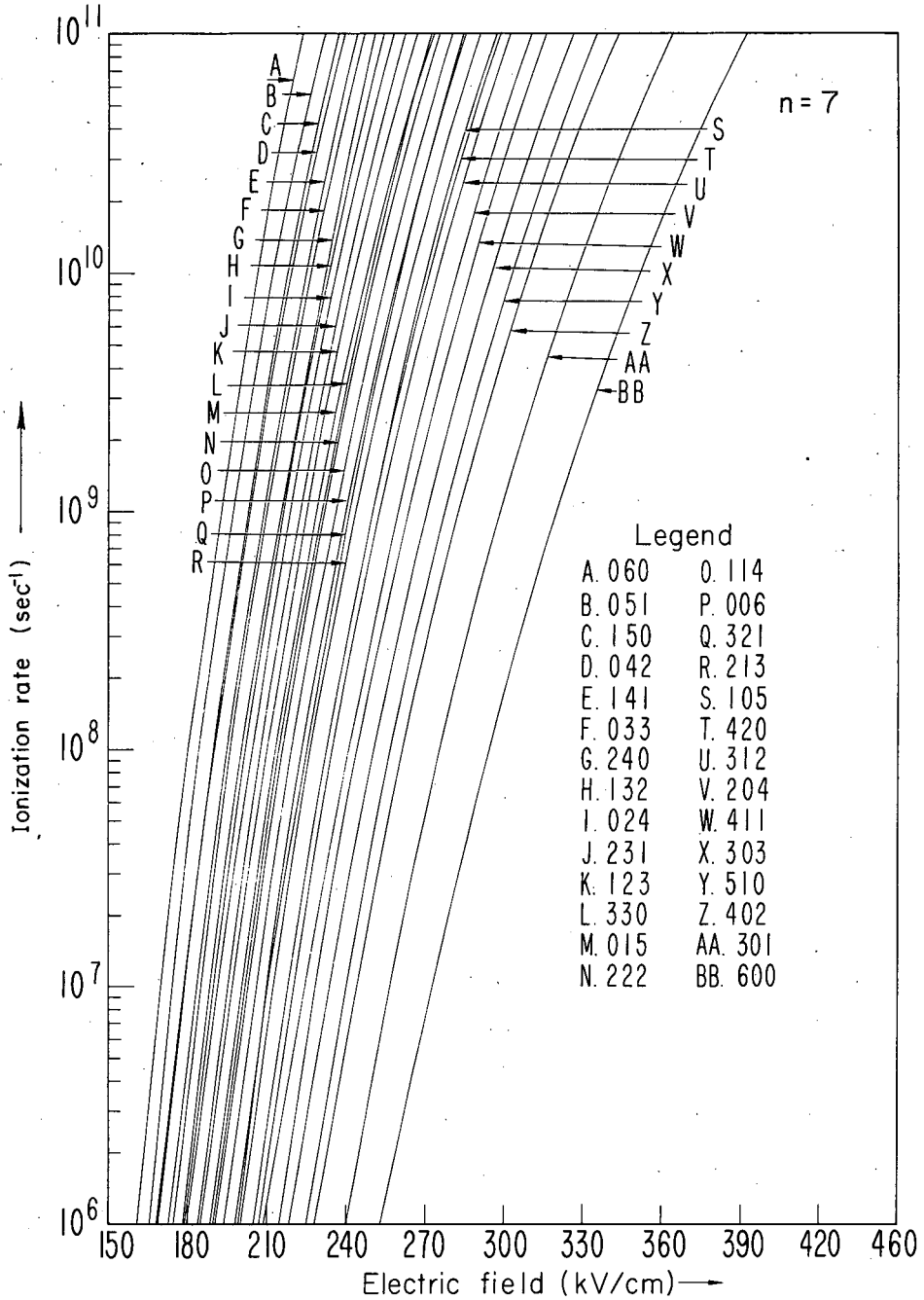

* see errata on above.

Fig. 3. Ionization rate vs field strength for all Stark states of the level n = 7 (from Ref. 7). The numbers in the legend are the parabolic quantum numbers (n_1, n_2, m).

B. Inelastic Collisions of Hydrogen Atoms

1. Theoretical Models

Most of the cross sections for inelastic collisions of excited hydrogen atoms have been evaluated in the first Born approximation (FBA).[12, 14, 16] This is essentially a first-order perturbation-theory description of the collision process, in which it is assumed that the incident projectile is described by a plane wave that is diffracted only slightly by the target. If the scattering potential is of the order V_0 and is effective over a region a, the condition for the validity of the FBA can be expressed as $V_0 a/\hbar v << 1$, where v is the impact velocity.[12] For a Bohr atom this means that the relative velocity of the colliding particles must be much greater than the orbital velocity of the electron in the target atom [$v >> 2 \times 10^8$ cm/sec for collisions with H(1s)].

The result of the FBA for a transition from an initial state p to a final state q is given by[16]

$$\sigma(p \to q) = \frac{M^2 v_q}{2\pi\hbar^4 v_p} \int_{-1}^{1} \left| \langle p | V | q \rangle \right|^2 d(\cos\theta), \qquad (1)$$

where $\langle p|V|q\rangle$ is the interaction potential averaged over the initial and final states of the system, v_p and v_q are the velocities of relative motion when the states p or q are occupied, M is the reduced mass of the system, and θ is the angle between v_p and v_q.

For H-H collisions, for example, the states $|p\rangle$ and $|q\rangle$ are expressed as a product of a plane wave describing the relative motion and the hydrogenic wave functions describing each atom. Thus the matrix element can be expressed as

$$\langle p|V|q\rangle = \int d\underset{\sim}{R} \langle 1, 2|V|1', 2'\rangle (\underset{\sim}{R}) \exp(i\underset{\sim}{K} \cdot \underset{\sim}{R}) \qquad (2)$$

Here $\underset{\sim}{R}$ is the position of the projectile relative to the target, $\underset{\sim}{K} = \underset{\sim}{k}_p - \underset{\sim}{k}_q$ is the change in the momentum of the projectile caused by the collision, and $\left\langle 1,\ 2 \left| V \right| 1'2' \right\rangle (\underset{\sim}{R})$ is the interaction potential averaged over the hydrogenic wave functions describing the two colliding atoms before and after the collision.[16]

For computational purposes it is often convenient to express the integration variable θ of Eq. (1) in terms of the change of momentum $\underset{\sim}{K}$. The range of integration is then determined by the changes in momentum allowed by conservation of energy and momentum.[16]

A simplified version of the FBA, known as the Bethe or dipole approximation, can be obtained by making the substitution $\exp(i\underset{\sim}{K}\cdot\underset{\sim}{R}) \approx 1 + i\underset{\sim}{K}\cdot\underset{\sim}{R}$ in Eq. (2). This approximation tends to overestimate the contributions for large momentum transfer $\underset{\sim}{K}$ (long-interaction times), so a cutoff K_c, deduced from known FBA results, is usually introduced.[19-24, 33] The general form of the Bethe approximation for excitation by electron impact is given by[24]

$$\sigma(n,\ \ell \rightarrow n', \ell') = \pi a_0^2 \frac{C(n, \ell, n', \ell')}{E} \ell n\, D(n, \ell, n'\ell')\, E, \qquad (3)$$

where E is the electron-impact energy, D is a function of the cutoff momentum and the energy difference between the levels, and C is a function of the orbital angular momentum ℓ and the dipole matrix element connecting the states. This approximation has been shown to agree with FBA results to within ±10% for electron collisions when the incident energy is greater than 15 times the threshold energy.[21-24]

Recently, a semiclassical model for inelastic collisions has been proposed by Seaton.[34] In this impact-parameter method, he assumes classical rectilinear trajectories for the projectile and calculates quantum-mechanical transition probabilities by first-order time-dependent perturbation theory. These are then integrated over

all impact parameters; special corrections are made for impact parameters that are smaller than the radius of the orbit under consideration. The results of this model are in agreement with FBA calculations at high energies and with experimental results at low energies.

2. Collisional Excitation

a. e-H collisions

Cross sections for excitation by electron impact of the excited levels accessible in this experiment (n = 6 to 9) have been calculated in the first Born, Bethe, and impact-parameter approximations.[21-24,34-38] The results of Milford and co-workers,[24] which were worked out partly in the first Born and partly in the Bethe approximation, are presented in Fig. 4. Their coefficients $C(n,\ell,n',\ell')$ and $D(n,\ell,n',\ell')$ were used to evaluate Eq. (3) for $E = 5425$ eV, which is the kinetic energy of an electron of the same velocity as the 10-MeV H^0 beam of this experiment. Calculations for the $n = 3$ to 4 transitions were carried out for all possible values of $\Delta\ell = \ell' - \ell$, and it was found that transitions with $\Delta\ell = 1$ were the largest by at least an order of magnitude.[21] Subsequent FBA or Bethe calculations for higher states were therefore carried out only for $\Delta\ell = 1$, and only these transitions are shown in Fig. 4. Notice that: (a) for a given level n, the nearly circular (large ℓ) orbits are most easily excited; (b) excitation cross sections increase very rapidly with n; and (c) transitions with $\Delta\ell = 1$ and $\Delta n = 1$ dominate by almost an order of magnitude.

Since the present experiment cannot resolve the individual states of a level n, we are particularly interested in cross sections for transitions from n to n' that have been statistically averaged over the states of each level. We use the symbol $\sigma_{n,n'}$ for these averaged cross sections. In Table I we compile the theoretical results found in the literature for $\sigma_{n,n'}$ due to electron impact. The table is arranged in the form of a matrix. All numbers above the diagonal ($n' > n$) are

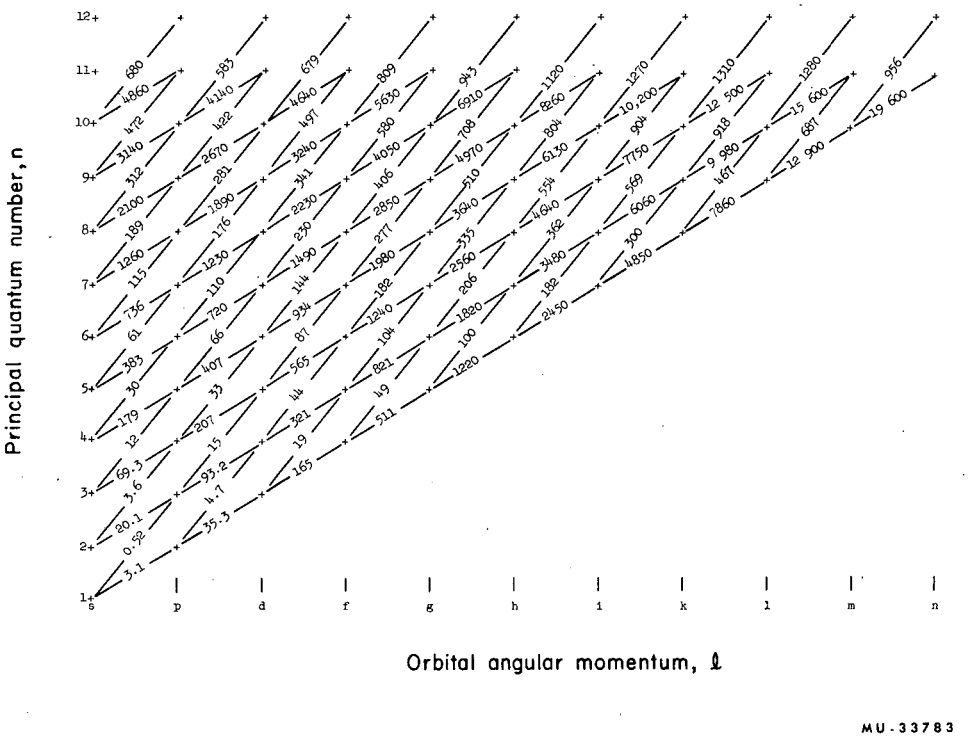

Fig. 4. Collisional excitation cross sections for 10-MeV hydrogen atoms incident on an electron target, based on the results of McCoyd and Milford.[24] The numbers on the lines connecting the various states are the cross sections for the indicated $n, \ell \rightarrow n+1, \ell+1$ or $n, \ell \rightarrow n+2, \ell+1$ transition, in units of 10^{-18} cm^2. (Theoretical)

n \ n'	1	2	3	4	5	6	7	8	9	10	11	12
1		3.1[a] 3.2[b] (3.6[c])	0.52[a] (0.63[c])	(0.22[c])	(0.11[c])	(0.058[c])	(0.035[c])	(0.023[c])	(0.016[c])	(0.012[c])		
2	0.9		32[a] 31[b] (53[d])	4.5[a] (6[d])	(3[d])	(1[d])	(0.6[d])	(0.4[d])	(0.3[d])	(0.2[d])		
3	0.06	15		130[a] 130[b]	17[a]							
4	0.014	1.1	74		374[a] 368[b]	43[a]						
5	0.004	0.5	7	240		846[a] 835[b]	93[a]					
6	0.002	0.1		12	588		1650[a]	175[a]				
7	7×10^{-3}	0.05			47	1210		3070[a]	300[a]			
8	4×10^{-4}	0.03				98	2350		4990[a]	481[a]		
9	2×10^{-4}	0.01					181	3930		7870[a]	749[a]	
10	1×10^{-4}	0.01						308	6370		11 900[a]	1080[a]
11									501	9830		
12										750		

Table I. Excitation cross sections, $\sigma_{n,n'}$, for collisions of 10-MeV hydrogen atoms with electrons. (Theoretical) All entries are in units of 10^{-18} cm^2.

a. McCoyd and Milford[24]
b. Seaton[35]
c. McCarroll[36] (extrapolated values)
d. Statistical average over states of the results of McCrea and McKirgan[37] and of Boyd[38] (extrapolated valued)

cross sections for excitation, those below the diagonal ($n' < n$) for de-excitation (Sec.. II. B. 3). All entries are in units of 10^{-18} cm^2. They have been evaluated at electron energies of 5425 eV; brackets indicate where extrapolation of published results was required. A detailed description of the construction of Table I is given in Appendix C.

This table clearly demonstrates the large cross sections predicted for transitions in which $\Delta n = 1$. Cross sections with $\Delta n = 2$ are typically only a tenth as large; for larger values of Δn the cross sections decrease less rapidly, dropping off approximately by a factor of 2 for each unit increase of Δn. A strong dependence on n is also clearly demonstrated; for example, the cross section for excitation by $\Delta n = 1$ can be approximated by the expression $\sigma_{n,n+1} \approx 2 \times n^{3.8}$ for $n > 3$. The many vacancies in the table show that this field is still open for further theoretical investigation.

b. H-H collisions

The only published results for collisions of excited hydrogen atoms with other hydrogen atoms are the FBA results of Bouthilette, Healy, and Milford (BHM).[25] The BHM calculations are for collisions of the type

$$H(n,\ell) + H(1s) \rightarrow H(n+1,\ell') + H(2s \text{ or } 2p). \qquad (4)$$

This, of course, describes only one of the many collision processes that result in the excitation of the level n to the level $n+1$. Since the target atom may be excited, ionized, or remain in the ground state, a complete description of the n to $n+1$ excitation requires consideration of the processes

$$H(n,\ell) + H(1s) \rightarrow H(n+1,\ell') + H(n'',\ell'') \qquad (5)$$

and

$$H(n,\ell) + H(1s) \rightarrow H(n+1,\ell') + H^+ + e^- \qquad (6)$$

for all n'' and ℓ''. In fact, results for H(1s) - H(1s) collisions[16]

would indicate that some of these other processes, especially the one that leads to ionization of H(1s) [Eq. (6)], may be as important as Reaction (4). Nevertheless, the results of BHM illustrate some important differences between H-H and H-e collisions; they have therefore been tabulated in Table II. Comparing these partial results for H-H collisions with the H-e collisions of Fig. 4, we note that the H-H cross sections are predicted to be smaller by more than 2 orders of magnitude and that they do not show a strong dependence on n. (The cross section for $\langle 2\text{-}3 \rangle_\ell$ is larger than that for $\langle 3 - 4 \rangle_\ell$ because of the inclusion of the 2s - 3d term in the average over ℓ.) Further calculations are required before any definite conclusions can be drawn.

3. Collisional De-excitation

The cross section for de-excitation from n' to n (n' > n) is related to the cross section for excitation from n to n' by the equation

$$n^2 v_p^2 \sigma_{n,n'} = n'^2 v_q^2 \sigma_{n',n} , \tag{7}$$

in which v_p and v_q are the relative velocities before and after the $n \rightarrow n'$ collision. [See Appendix D for a derivation of Eq. (7)].

At high energies the change in velocity resulting from the collision is negligible. Setting $v_q = v_p$, we obtain

$$\sigma_{n',n} = \frac{n^2}{n'^2} \sigma_{n,n'} . \tag{8}$$

This relation has been used to compute the de-excitation cross sections (n' < n) from published excitation cross sections (n' > n) (cf. Table I).

4. Collisional Ionization

The ionization of excited states of hydrogen by electron impact for the levels $n \geq 3$ is currently under consideration.[39,40]

Table II. Cross sections (10^{-18} cm^2) for hydrogen-hydrogen collisions in which one atom undergoes the indicated transition while the other atom is excited from n = 1 to 2. Results of BHM[25] extrapolated to 10 MeV.[a] (Theoretical). See errata on this

Transition	Cross section	Transition	Cross section
2s - 3s	0.007	3s - 4p	0.010
2s - 3p	0.011	3p - 4d	0.017
3s - 3d	0.028	3d - 4f	0.052
2p - 3s	0.001	$\langle 3\text{-}4 \rangle_\ell^b$	0.035
2p - 3p	0.009	4s - 5p	0.009
2p - 3d	0.037	4f - 5q	0.058
$\langle 2\text{-}3 \rangle_\ell^b$	0.047		

a. These results, which were evaluated by BHM up to energies of about 1 MeV, indicated an E^{-1} dependence at high energies and were extrapolated accordingly.

b. The values $\langle n - (n+1) \rangle_\ell$ are statistically weighted averages of the $n, \ell \rightarrow n+1, \ell'$ cross sections shown in the table.

Only Bethe approximation results by Stauffer and McDowell[39] are available at present for the levels of interest here. For the levels n = 1 to 3, for which a comparison with other results can be made, these calculations are in rather poor agreement with FBA results. In the high-energy region, for example, where agreement between FBA and experiment has been established for ionization of the ground state,[14,41] the Stauffer and McDowell results are approximately 1/3, 1/5, and 1/4 as large as FBA results for the levels n = 1, 2, and 3 respectively.[39,40,42-44] Having warned the reader of this discrepancy, we present the results of Stauffer and McDowell for n = 3 to 10 in Table III. These values were obtained by extrapolation from 200 to 5425 eV.

Even though the magnitudes may be too small by a factor of 4 or 5, a comparison with the excitation cross sections of Table I shows that the ionization cross sections have a much weaker dependence on n. Whereas $\sigma_{n,\,n+1}$ was found to be proportional to $n^{3.8}$ at this energy, the ionization cross section $\sigma_{n,\,C}$ seems to be proportional to the first power of n. A weak-n dependence is also indicated in the FBA results of Omidvar and Sullivan.[40] Although excitation and ionization cross sections are comparable for the ground state,[14] the cross sections for excitation of the higher levels are much greater than those for ionization.

Theoretical estimates for ionization of excited levels of hydrogen by collisions with other hydrogen atoms have not been reported.

Table III. Cross sections for ionization of 10-MeV excited hydrogen atoms by electron impact in units of 10^{-18} cm^2. Extrapolations of Stauffer and McDowell.[39] (Theoretical).

n	3	4	5	6	7	8	9	10
$\sigma_{n,C}$	10	13	18	22	26	30	34	39

III. EXPERIMENTAL APPARATUS AND PROCEDURE

A. Production of 10-MeV Excited Hydrogen Atoms

The over-all experimental arrangement is shown schematically in Fig. 5. The Berkeley heavy-ion linear accelerator (Hilac) was used to produce a beam of 20-MeV H_2^+ ions. This beam was bent 15° to remove possible contaminants and was partially dissociated by collisions in the first gas cell. Of the two modes of collisional dissociation,

$$H_2^+ \rightarrow 2H^+ + e^- \tag{9}$$

and

$$H_2^+ \rightarrow H^+ + H^0(n, \ell) , \tag{10}$$

the second produces 10-MeV atoms with a population distribution covering all excited levels.[45,46] Since only the atoms were of interest, the charged particles, H^+ and H_2^+, were swept out of the beam with magnet LM1. The reasons for using this particular method to produce a neutral beam are discussed in Appendix E.

The first gas cell was identical to the gas-target chamber that is described in detail in Sec. III. B. 1. It was usually filled with H_2 gas at a pressure of 2×10^{-2} torr. This gave a good yield of neutral atoms and made it possible to maintain the adjacent drift section at less than 10^{-5} torr.

The magnet LM1 not only swept out the ions, but also Lorentz ionized the highly excited neutral atoms. The minimum field required to sweep out the ions was 2 kG ($\underset{\sim}{F} = \underset{\sim}{v} \times \underset{\sim}{B}$ = 88 kV/cm), which is sufficient to Lorentz ionize all levels above n = 10. The field could be increased to a maximum of 22 kG (961 kV/cm), which is sufficient to Lorentz ionize most of the n = 5 level (see Fig. 2). By an appropriate choice of the field strength, it was thus possible to prepare a beam of hydrogen atoms in which only the excited levels n = 1 to n^* were populated; n^* could be varied from 4 to 10.

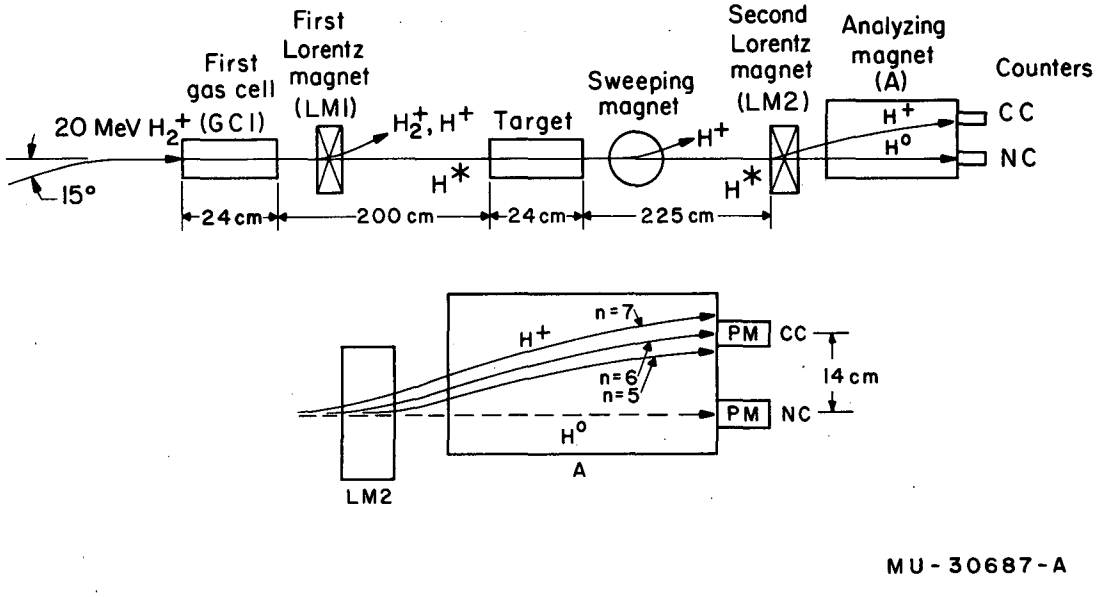

Fig. 5. Diagram of the experimental arrangement.

The magnetic fields of LM1, LM2, and A were monitored by Hall probes taped to the pole faces. These were calibrated against the mid-plane field measurements by a Rawson rotating-coil gaussmeter.

A photograph of the apparatus for the production of the neutral beam is shown in Fig. 6. On the left is the first gas cell, followed by magnet LM1. The pump on the right maintained the drift section at base pressure. Faraday cups could be introduced at this point for alignment purposes.

B. Targets

1. Gas Target

The neutral beam passed through a 200-cm drift section and then entered the target section. Either a differentially pumped gas cell or a weakly ionized Philips ionization gauge (PIG) type discharge could be used. The gas cell is illustrated in Fig. 7. It consisted of a high-pressure target chamber and an intermediate pressure region backed by a 1500 liter/sec oil-diffusion pump; this pump had a water-cooled cap to minimize backstreaming. To obtain maximum pumping speeds no other baffles were used. All other pumps used in this system were oil-diffusion types with liquid-nitrogen-cooled baffles.

The connecting tubes aided in maintaining the pressure differential. It was possible to maintain in the intermediate region a pressure that was only about a hundredth that of the pressure in the target chamber, and the pressure in the drift sections was about a hundredth that of the intermediate region. For example, when the pressure in the target section was 5×10^{-2} torr, the pressure in the drift sections was approximately 5×10^{-6} torr.

The valve between the high- and intermediate-pressure regions was used to hasten initial pumpdown. A base pressure of 1×10^{-6} torr could be achieved. During operation the valve was closed and hydrogen

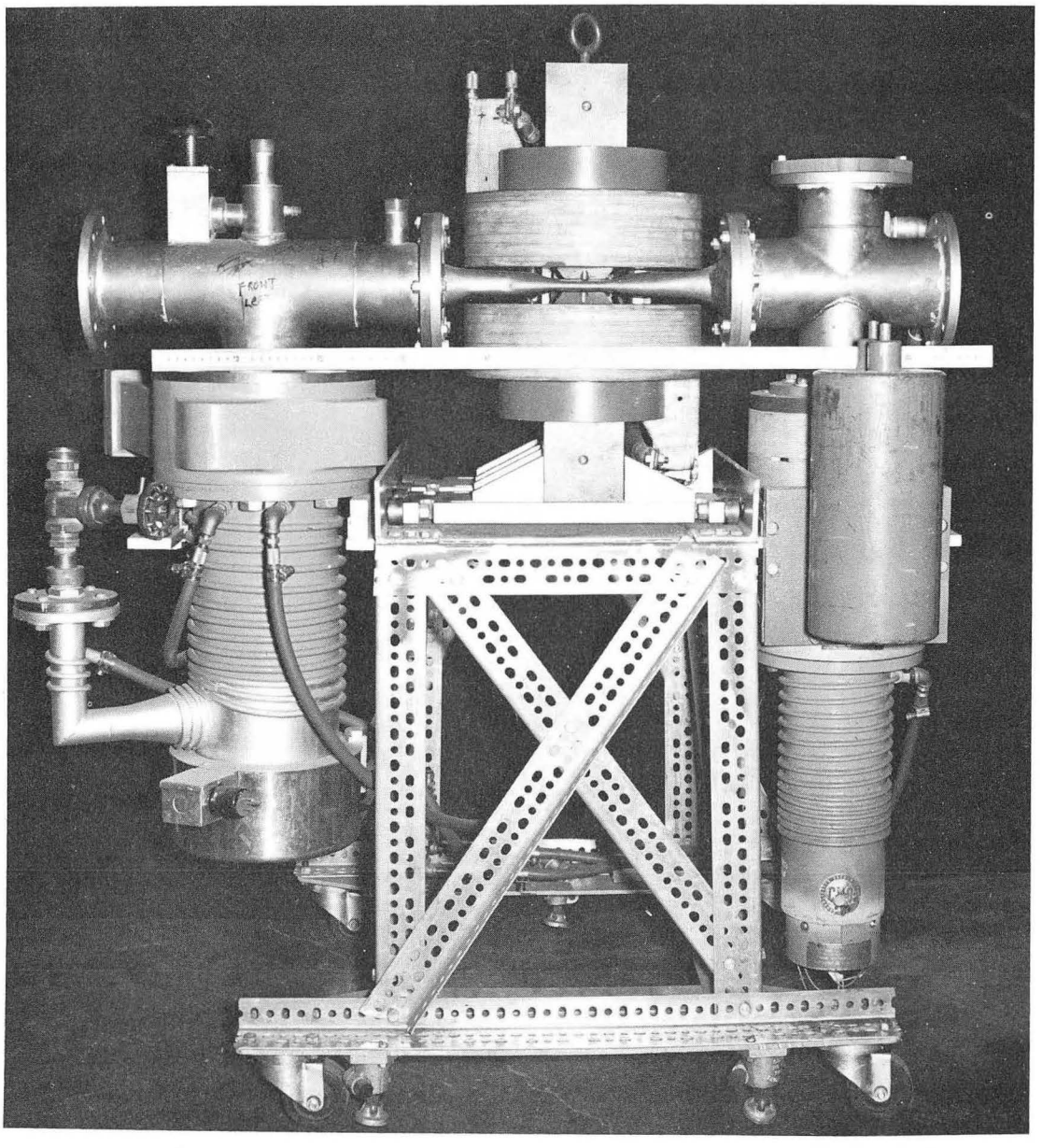

ZN-4197

Fig. 6. Photograph of the apparatus for the production of the neutral beam. The molecular-ion beam, incident from the left, is partially neutralized in the first gas cell. All ions are swept out of the beam by magnet LM1 (center). This magnet also Lorentz ionizes all levels above a predetermined n^*. The pump on the right maintains the adjacent drift section at base pressure.

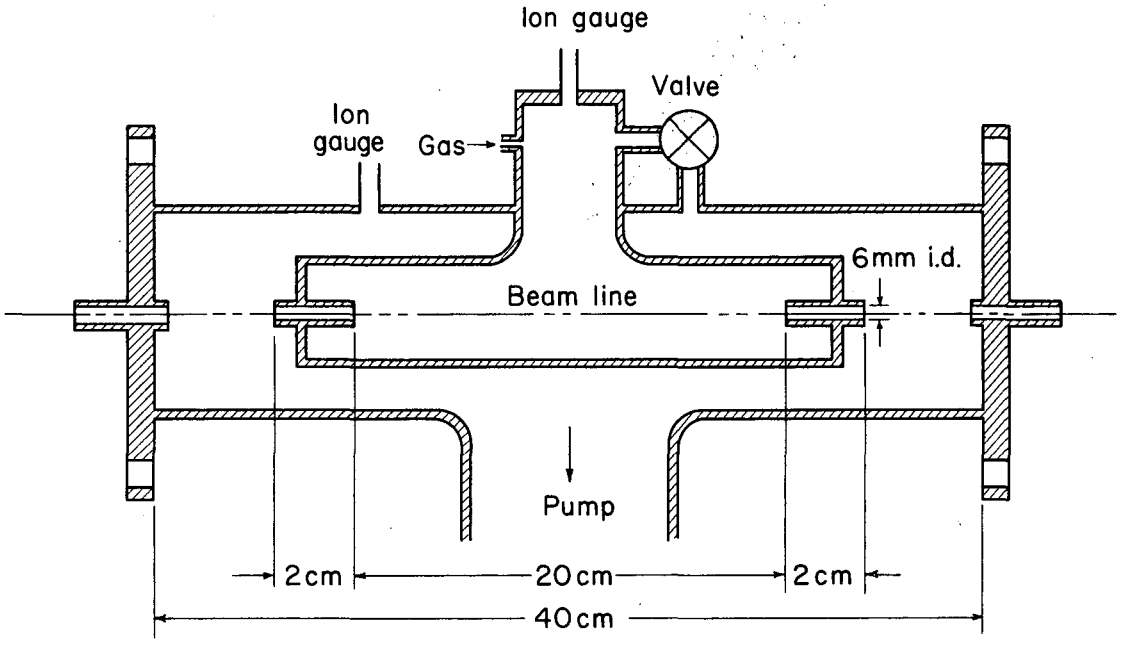

Fig. 7. Diagram of the gas target.

gas was continuously bled through the chamber. The gas was obtained from a cylinder of commercial high-purity gas. No further purification was attempted. Typical operating pressures ranged from 1×10^{-3} to 5×10^{-2} torr.

A linear pressure drop in the connecting tubes was assumed, and the effective length of the target chamber was taken to be 24±1 cm, the distance between the midpoints of the connecting tubes.

The pressure in the target chamber was monitored by a Westinghouse Type 7676 high-pressure ionization gauge (Schulz-Phelps type). This was cross calibrated with three liquid-nitrogen-trapped McLeod gauges; the McLeod gauge readings, at best, agreed within 5%. This uncertainty of the absolute accuracy of the McLeod gauges and fluctuations in the calibration from day to day indicate an uncertainty of ±10%.

2. Weakly Ionized Target

For the study of collisions with charged particles, the gas target was replaced by a PIG discharge, a diagram of which is shown in Fig. 8. A photograph of the partially assembled chamber, showing the microwave horns and Langmuir probe (introduced from the top) used for density measurements, is presented in Fig. 9.

The field coils provided an axial magnetic field of the order of 200 gauss. The brass central chamber, maintained at ground potential, served as the anode. Two oxidized-aluminum disks, insulated from the anode by 5-cm glass sections, served as cold emission cathodes.

The beam from the Berkeley Hilac comes in 3-msec pulses, 12 to 20 times a minute. Consequently, the discharge could be operated on a pulsed basis. A potential negative with respect to the anode, typically 500 volts, was applied 1 msec before the beam pulse arrived and was maintained for 5 msec. The discharge current during this time was approximately 1 ampere. The discharge was operated in hydrogen over a pressure range from 2×10^{-3} to 2×10^{-2} torr; again

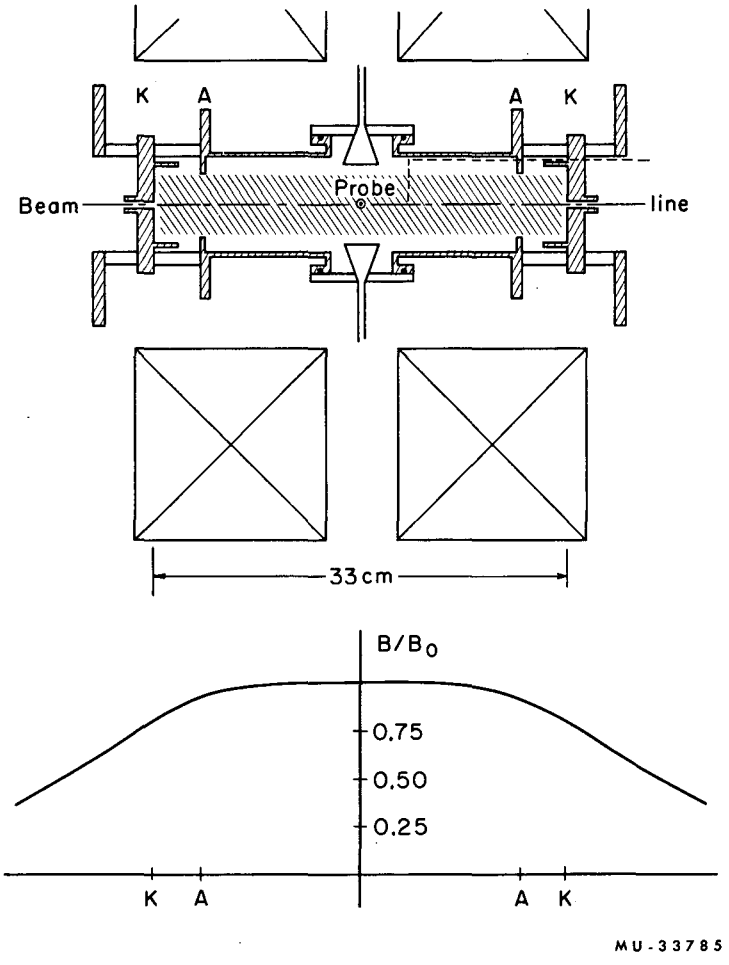

Fig. 8. Diagram of the PIG discharge-target chamber (drawn to scale). The dashed line indicates the shape of the right-angle probe used for longitudinal density measurements (Fig. 11); it was located at an azimuth of 45° to clear both the radial probe and the microwave horns. The curve below the diagram shows the shape of the magnetic field produced by the coils.

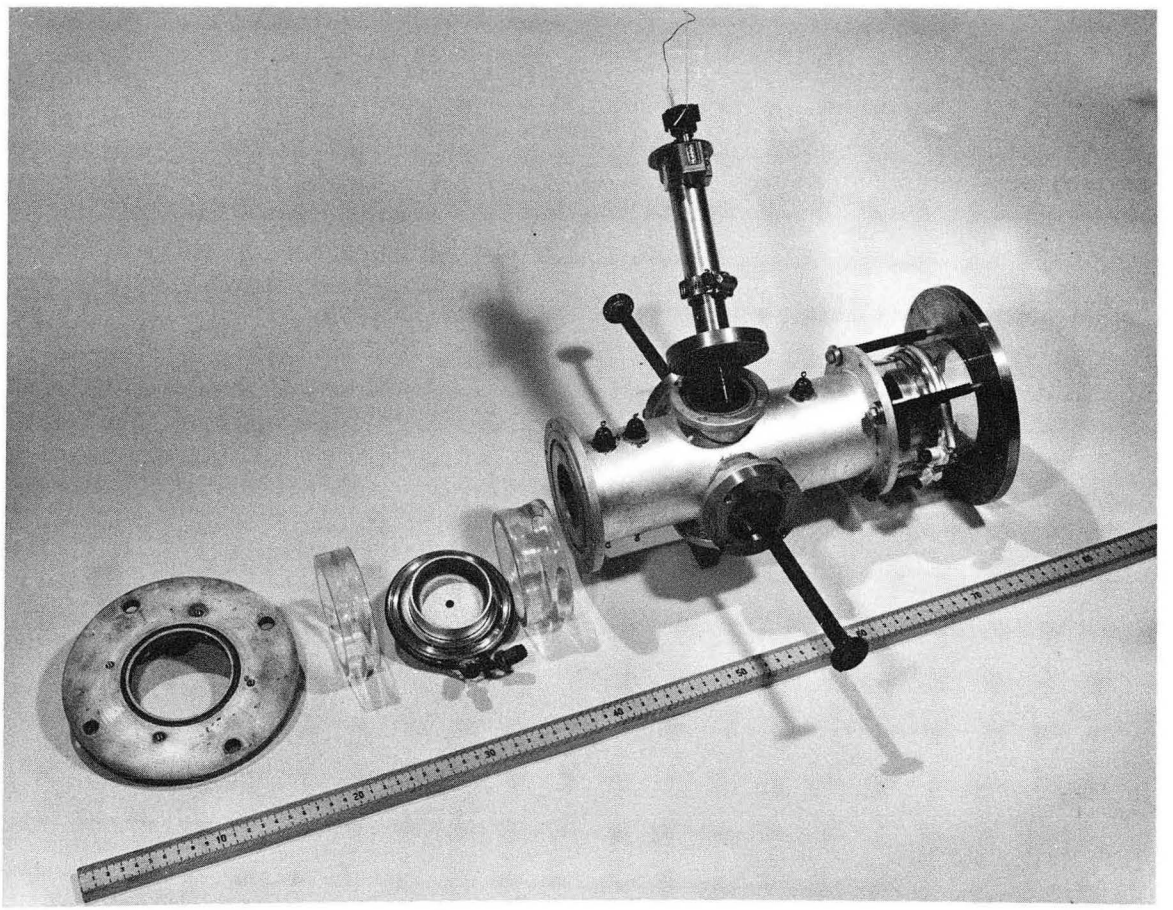

ZN-4199

Fig. 9. Partial assembly of PIG discharge-target chamber, showing the microwave horns and radial probe (introduced from the top) used for density measurements.

the gas was continuously bled through the chamber. Both the applied voltage and the pressure were varied to achieve a range of electron densities. A maximum of 1% ionization could be attained.

The electron density was measured both with Langmuir probes and 8-mm microwaves. The radial probe (see Fig. 9), a 0.51-mm diameter tungsten wire protruding 2.2 mm beyond a quartz envelope, was introduced into the chamber through a Wilson seal. This could be used to obtain radial profiles for the electron density and temperature.[47] The results for one set of operating parameters are shown in Fig. 10.

The 8-mm microwaves were transmitted along a diameter (Figs. 8 and 9), and the density was deduced from a phase-shift analysis[48] and the shape of the radial electron distribution (Fig. 10).

For the excitation experiments the radial probe was located 1.25 cm from the axis. The probe was biased to -200 V with respect to the anode, and the saturated ion current was monitored. With the assumption that $T_e \approx 0.7$ eV (Fig. 10), the electron density at $r = 1.25$ cm was deduced from the saturated ion current; the density on the axis was then obtained by correcting for the radial profile (multiplying by 2.2/1.5, see Fig. 10).

The density was simultaneously monitored with microwaves. The probe measurements were usually 30% lower than the phase-shift analysis. The two measurements were averaged, and an uncertainty of ± 25% was assigned to the average value. With the assumption of charge neutrality, the charged-particle density was taken to be twice the electron density.

To determine the effective length of the target chamber an axial-density profile is required. Such a measurement was attempted by introducing a Langmuir probe through one of the beam tubes. The resulting signal indicated that this probe perturbed the plasma considerably as it was moved in, and only the initial rise in the density could be deduced from this. To avoid perturbing the plasma on the

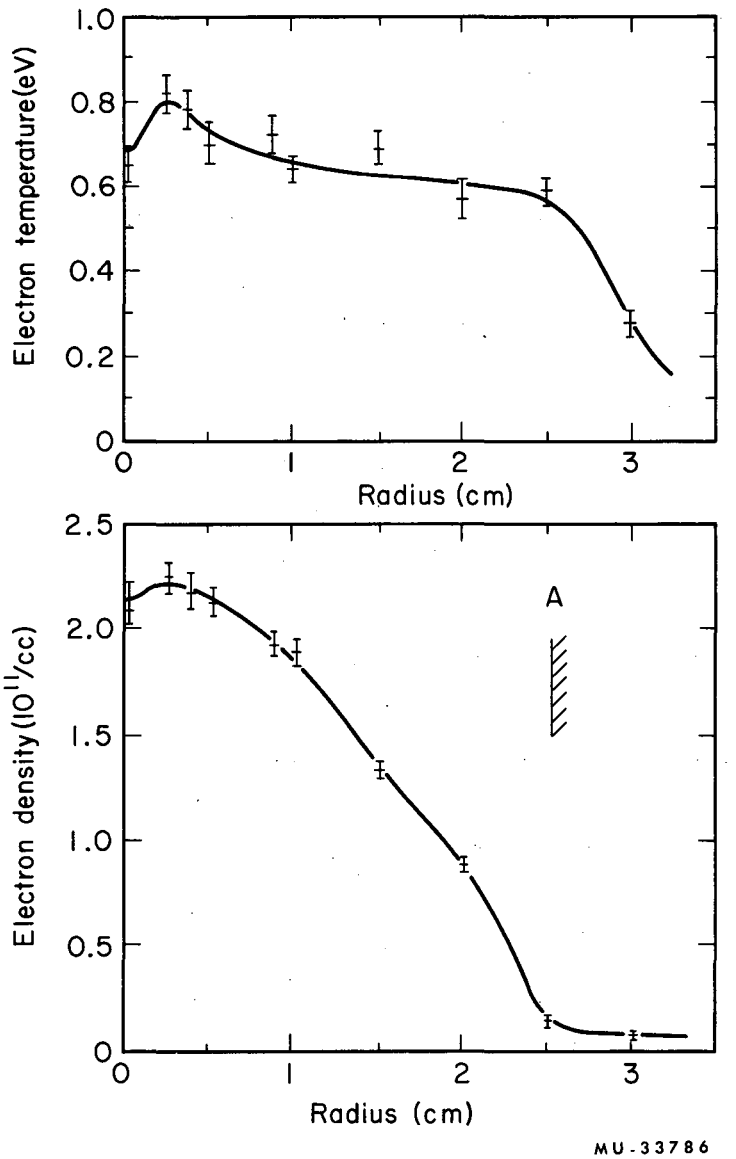

Fig. 10. Langmuir-probe measurements for the radial profiles of electron temperature and density in the PIG target. The error bars are based on reproducibility only (Hydrogen gas; pressure, 11×10^{-3} torr; applied potential, 400 V; discharge current, 1.3A; magnetic field at center, $B_0 = 260G$).

axis, a right-angle probe (indicated in Fig. 8) was introduced at a radius of 3.5 cm. This probe did not noticeably affect the discharge. A longitudinal-density profile is shown in Fig. 11. The right-angle probe was removed when the PIG was used as a target.

C. Measurement of the Population of the Excited Levels

1. Method

A 225-cm drift section, maintained at a pressure of 10^{-5} torr or less, connected the target with the analyzing section. In this region, a sweeping magnet removed the protons produced by ionizing collisions in the target. A large pole face (25-cm diam) on this magnet made it possible to remove the protons with a weak magnetic field (1.4 kG), thus minimizing the associated Lorentz ionization.

Magnets LM2 and A, together with the detectors NC and CC, were used to measure the population of the excited levels of the 5-mm diameter beam of neutral atoms. Magnet LM2, which has tapered pole faces, produces the field profile shown in Fig. 12. The Lorentz ionization of successively lower levels occurs sequentially in space as the beam passes through this nonuniform field. Consequently, the protons resulting from Lorentz ionization of levels of high n undergo larger deflections in the field of LM2 than those from lower levels. This process is illustrated in the inset to Fig. 5. The maximum field strength of LM2 is 18 kG, equivalent to an electric field of 787 kV/cm in the rest frame of the 10-MeV H^0. From Fig. 2 we see that this field is sufficient to Lorentz ionize some of the states of the $n = 5$ level and all states of the levels with $n > 5$ in the time that the beam spends in the field region.

The protons were steered to the counter CC by the analyzing magnet A. This field was varied to obtain a Lorentz-ionization profile, the spatial distributions of the protons resulting from Lorentz ionization in LM2 of various levels (Fig. 13). The resolution of the

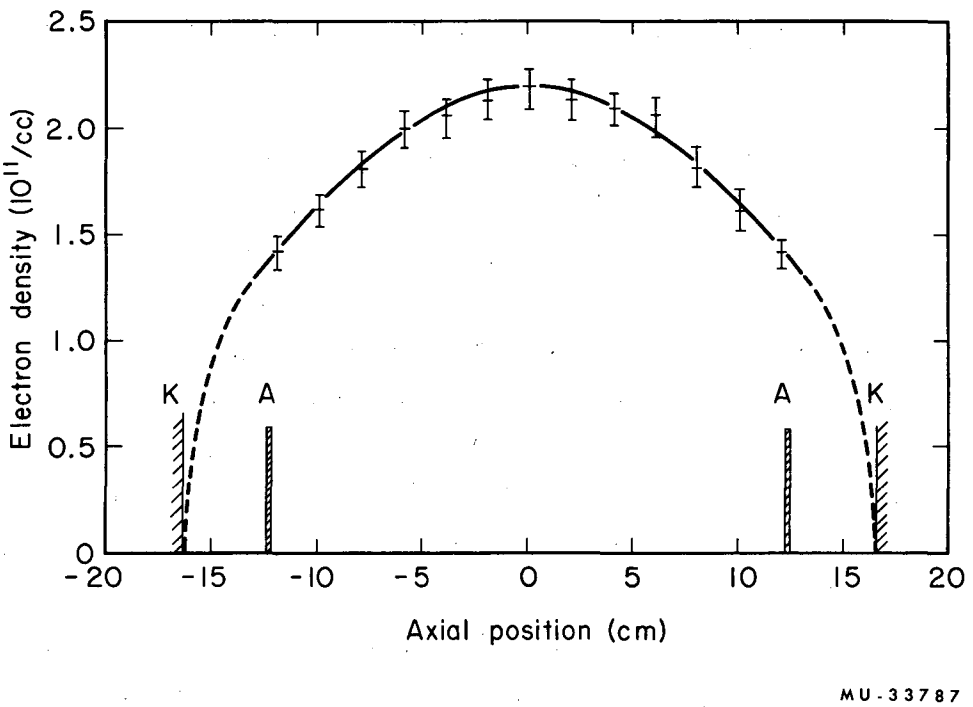

Fig. 11. Longitudinal profile of electron density in the PIG target, deduced from Langmuir-probe measurements. The dashed line is a best estimate for the region that was inacessible to the probe. The error bars are based on reproducibility only. The operating conditions are the same as for Fig. 10.

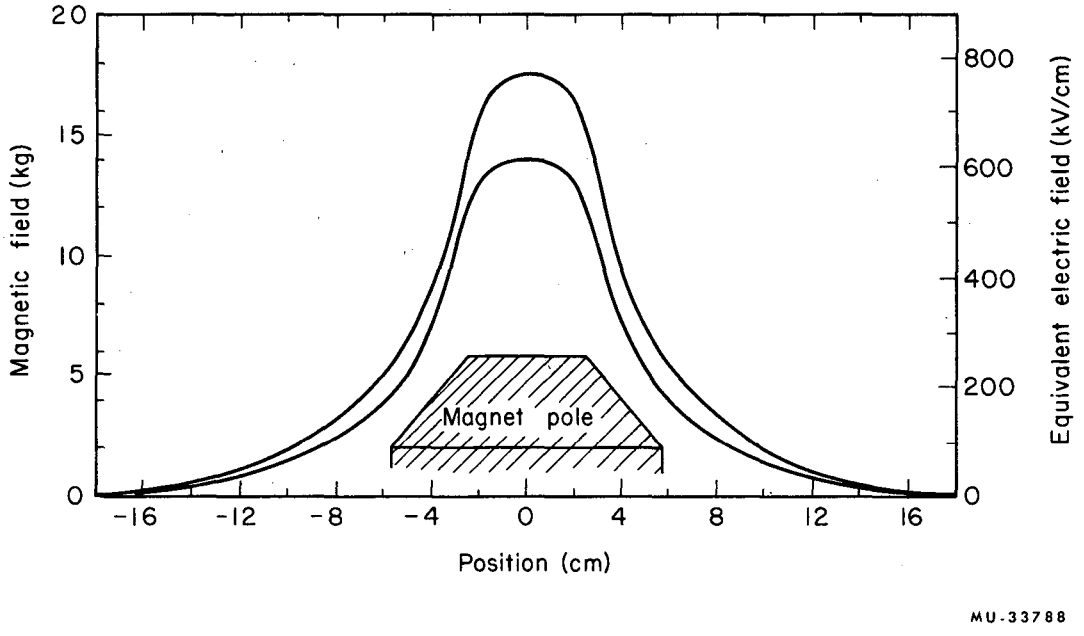

Fig. 12. Typical magnetic-field profiles, measured along the beam line, of magnet LM2 for two different field strengths.

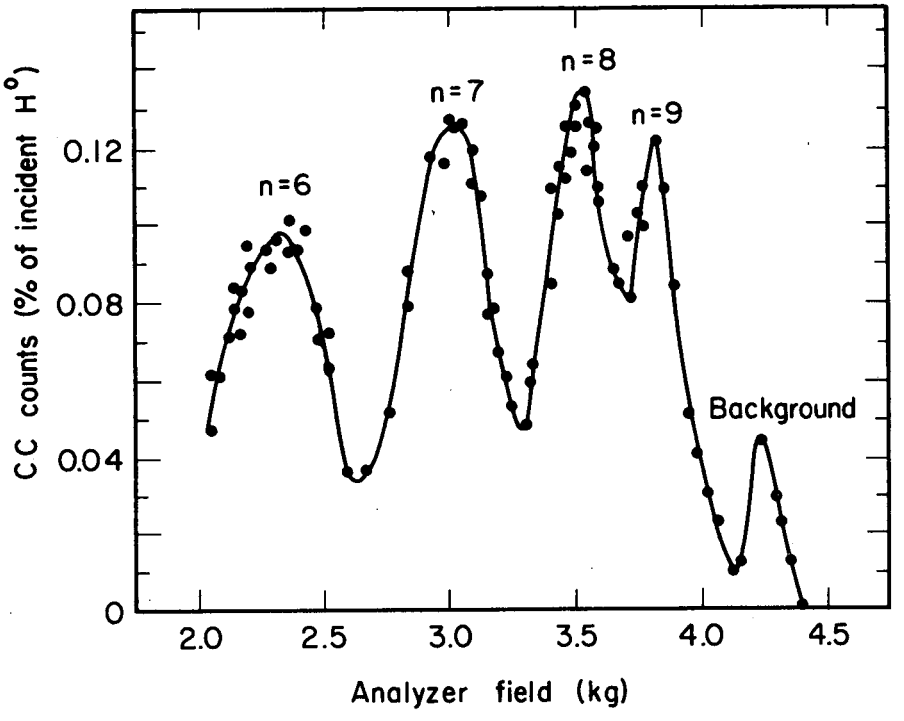

Fig. 13. Lorentz-ionization profile, measured with counters, for the excited levels $n = 6$ to 9 of hydrogen formed by collisional dissociation of H_2^+ in H_2. The peak labeled "Background" is due to ionization by collisions with the background gas in the drift section between the sweeping magnet and LM2. Pressure in first gas cell, filled with H_2: 24×10^{-3} torr; second gas cell $< 10^{-6}$ torr. Magnetic fields: LM1 = 0, LM2 = 13.85 kG (607 kV/cm), sweeping magnet = 1.6 kG (70 kV/cm, sufficient to Lorentz ionize levels with $n \geq 10$).

system was measured by stripping the neutral beam with a 6-μ Al foil, placed in various positions in the field of LM2, and sweeping the resultant proton beam with magnet A across two 3-mm-wide collimator slits, 22 mm apart, in front of CC. The dispersion, approximately 45 mm/kG, varied by 15% over the range of magnetic fields used in LM2. From a comparison of these trajectories with measured Lorentz profiles, it was estimated that the levels undergoing Lorentz ionization had an average lifetime in the field of approximately 2×10^{-10} sec.

The particles left the vacuum region through Al windows 125-μ thick and struck the detectors. Each of the detectors was a 5-cm-diam plastic scintillator connected by a 40-cm Lucite light pipe to a photomultiplier tube (RCA type 6810). The light pipe was needed to get the photomultiplier out of the fringe field of magnet A. The output of the photomultipliers was recorded by a scaler circuit.

A 3 mm by 40 mm collimating slit was used in front of the detector CC to obtain a good resolution of the Lorentz-ionization profile. The count rate was limited by the response time of the scalers and the very large neutral signal. To reduce the counting time, a perforated nickel plate, 0.27-mm-thick, was placed in front of the detector NC to attenuate the neutral-beam counts. This plate had 250 holes, each 0.08 mm in diameter, per square centimeter. It allowed 1 out of every 63 incident atoms to reach the detector, thus allowing the beam level to be raised. The analyzer section is shown in Fig. 14.

A pulse-height analysis of the photomultiplier signals was also made. This showed a very clean signal at 10 MeV, with some very low-energy noise. The discriminators were adjusted to remove this noise. When the perforated nickel plate was removed, it was found that $< 0.2\%$ of the pulses in the neutral detector corresponded to an energy transfer of 20 MeV; this sets an upper limit of 0.2% on the $2H^0$ or H_2^0 contamination of the H^0 beam.

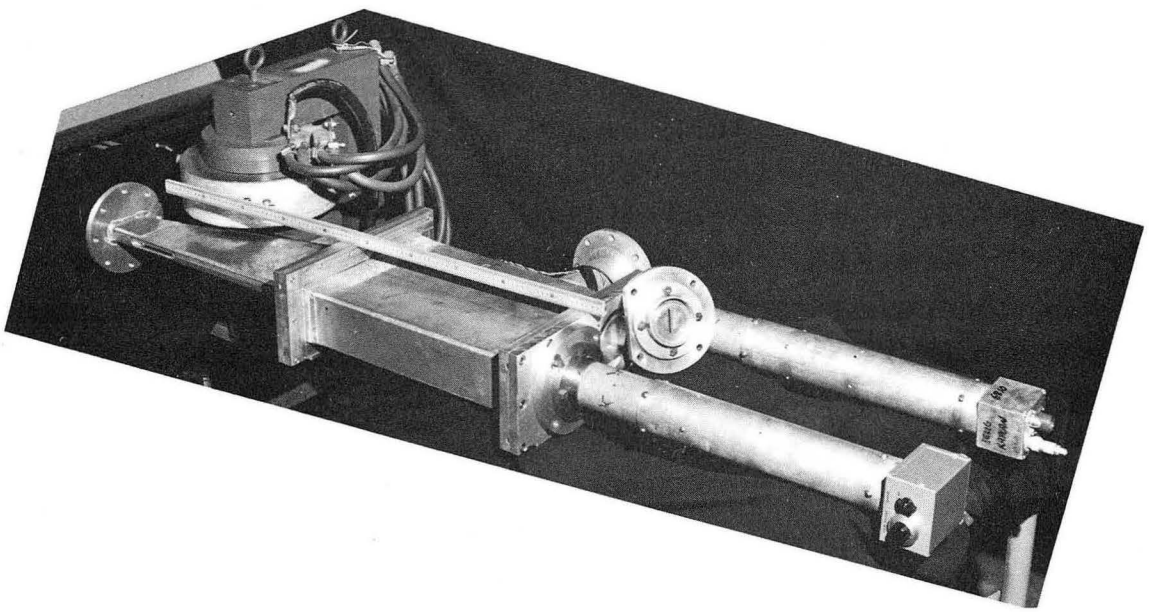

ZN-4198

Fig. 14 Analyzer section of the experiment. The excited atoms are Lorentz ionized in the nonuniform field of magnet LM2 (far left). The resulting protons are steered to the detector CC (partially assembled in the back of the picture). The remaining lowly excited atoms hit the detector NC (front of picture). The rectangular box (center) fits between the pole faces of the analyzer magnet A (not shown in figure). The flange in the rear leads to a liquid-nitrogen-baffled oil-diffusion pump. Emulsions could also be introduced through this port.

Since the PIG target was weakly ionized, it was desirable to separate out the effects of collisions with neutrals. This was accomplished by using the following technique. The PIG was pulsed on only during every second beam pulse. Two sets of scalers were used with each detector, and these were electronically gated such that one set recorded the data for the beam pulse when the PIG was on, the other when the PIG was off. The difference in these two readings was then due to collisions with charged particles in the hydrogen plasma. A block diagram of the circuit used for this technique is shown in Fig. 15.

The two sets of scalers were cross checked by disconnecting the PIG trigger and counting with each set for a gas target on alternate beam pulses. The signals always agreed within the counting statistics.

To check for possible errors due to rf pickup the PIG was pulsed, but the beam was intercepted ahead of the target; no counts were observed on either set of scalers. Thus no error was introduced by rf pickup.

Finally, the delay on the PIG trigger was decreased so that the beam passed through the target 500 μsec after the voltage pulse ceased. The agreement of this signal with the "PIG off" signal proved that the increase in counting rate when the discharge was on was indeed due to charged particles, and not due to impurities from the wall freed by the discharge.

An alternate scheme for determining the Lorentz ionization profile was to use a fixed field in magnet A and record the protons on a nuclear emulsion (Ilford K-2); the neutral counts were still monitored with the counter NC. The emulsions were introduced through the port visible in the rear of Fig. 14 and placed in a plane perpendicular to the beam. The developed emulsions were scanned with a low-power microscope. The density of tracks as a function of position showed the Lorentz-ionization profile (Fig. 16).

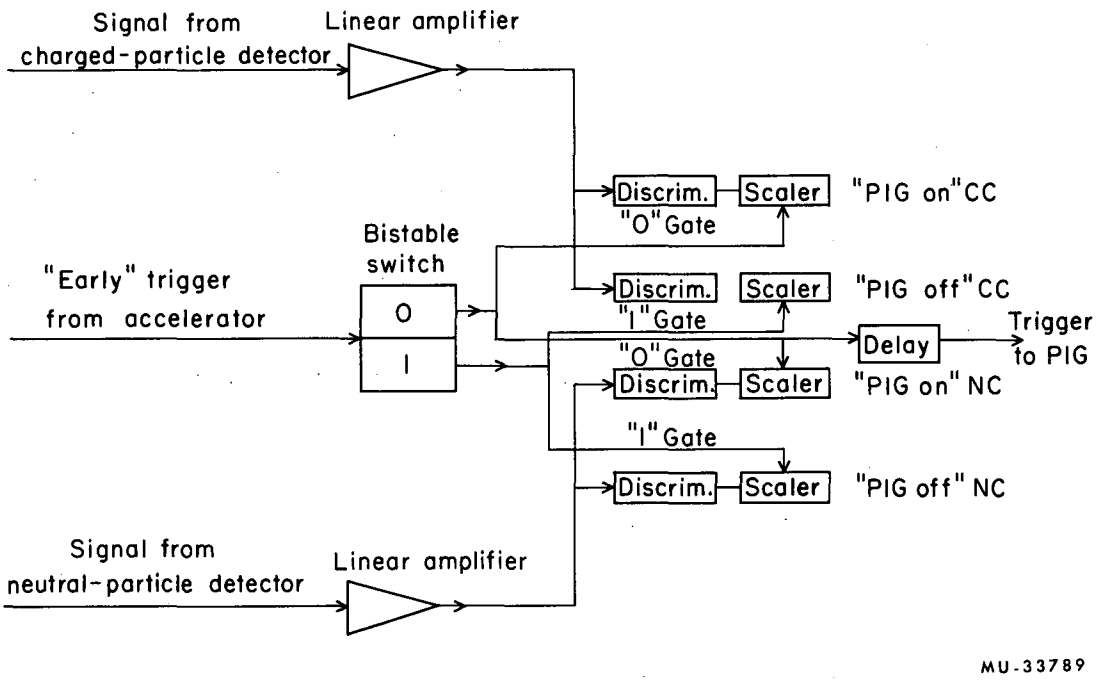

Fig. 15. Block diagram of the gating circuit used to separate out the effects of neutral collisions from the plasma target.

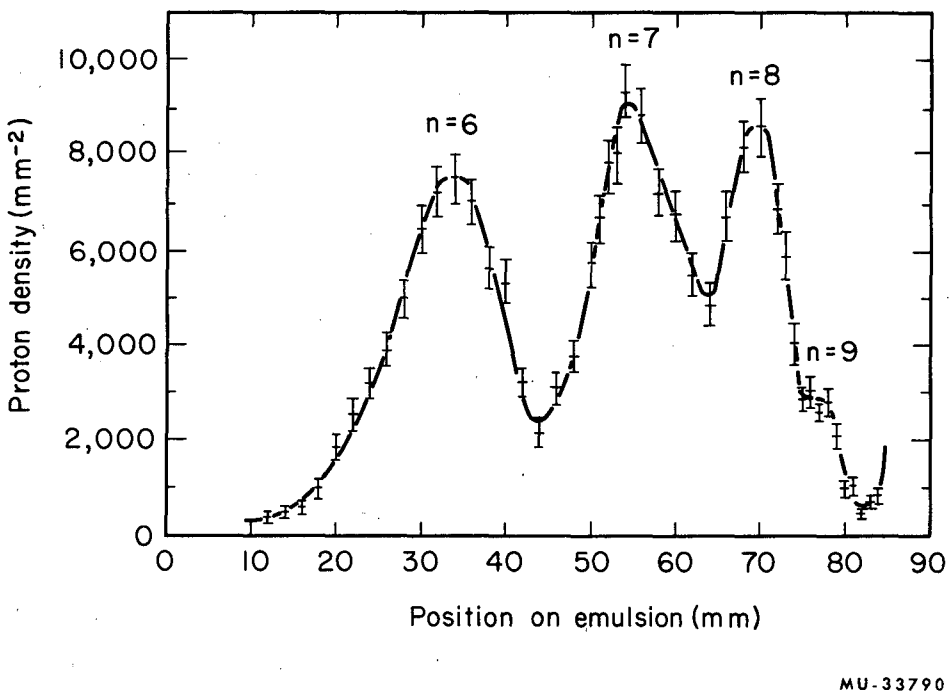

Fig. 16. A Lorentz-ionization profile, measured with a nuclear emulsion, for the excited levels n = 6 to 9 of hydrogen formed by collisional dissociation of H_2^+ in Ar. The particle density is based on the number of tracks in a 660 × 660 micron square. The n = 9 level appears as a small plateau at 7.7 cm because most of it was depopulated by Lorentz ionization in LM1. Pressure in first gas cell, filled with Ar: 44×10^{-3} torr; second gas cell < 10^{-6} torr. Magnetic fields: LM1 = 2.5 kG (109 kV/cm), LM2 = 13.85 kG (607 kV/cm), sweeping magnet = 1.6 kG (70 kV/cm), and magnet A = 2.55 kG (111 kV/cm). Total H^0 incident on target: 2.35×10^6.

2. Interpretation of the Lorentz Ionization Profile

The Lorentz ionization profiles (Figs. 13 and 16) resulted from the ionization of excited atoms at various positions in the non-uniform field of magnet LM2. When the target was evacuated, positive identification of the level n corresponding to each peak was obtained by observing the disappearance of individual peaks caused by Lorentz ionization as the magnetic field in LM1 was increased from 0. The disappearance of a particular peak was correlated with the predictions for strong-field ionization (Fig. 2) to determine the corresponding level.

The population of each excited level was obtained by integrating the corresponding peak of Fig. 13 and correcting for the finite width of the collimator.

Referring again to Fig. 13 we note that, although individual levels are resolved, there is no indication of any fine structure that would resolve the Lorentz ionization thresholds of individual states within the level. In an attempt to improve the resolution, the counter CC was replaced by a nuclear emulsion. The resulting Lorentz profile (Fig. 16) showed no improvement in the resolution, however.

To obtain the population of a level from the emulsions, a two-dimensional integration is required, one along the axis shown in Fig. 16 (the horizontal axis) and one at right angles (vertical). Vertical scans for randomly chosen horizontal positions on three different emulsions are shown in Fig. 17. These indicate that the vertical extent of the beam is uniform, so that the vertical integration has to be done only once.

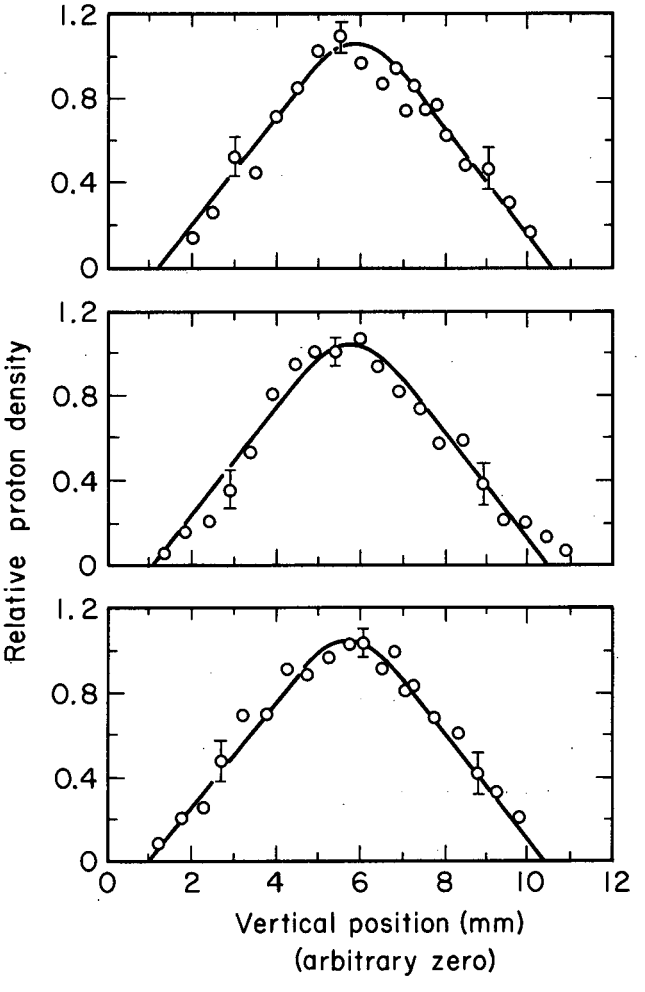

Fig. 17. Vertical scan of three different emulsions at random horizontal positions to determine the beam width. The lines are to guide the eye.

D. Collision-Induced Changes in the Population of Excited Levels

To determine changes due to collisional excitation in the population of the excited levels, LM1 was set to remove all incident atoms in excited levels above a predetermined value n^*. The repopulation of these levels was then observed as a function of the target thickness.

Collisional repopulation is demonstrated in Figs. 18 and 19. The first of these shows the changes in population due to collisions with H_2 for the case $n^* = 6$ as measured with emulsions. The three curves are representative of an evacuated target, a low-density target, and a high-density target. Figure 19 demonstrates the changes in population due to collisions with the plasma target for the case $n^* = 5$, as measured with counters. The poor resolution of the $n = 8$ and 9 peaks is typical for the observed repopulation of these levels.

In Tables IV and V we give the densities obtained by integrating these curves.

Note: The total incident beam was obtained by correcting the counts of NC for ionization losses in the target. For this correction the measured cross section $\sigma_{4901} = 2.2\times10^{-18}$ cm^2/molecule of H_2 was used for the gas target.[49] For the PIG target, we used an extrapolation of the experimental values of Fite and Brackmann for ionization by electron impact, $\sigma_{01} = 3.3\times10^{-18}$ cm^2.[15]

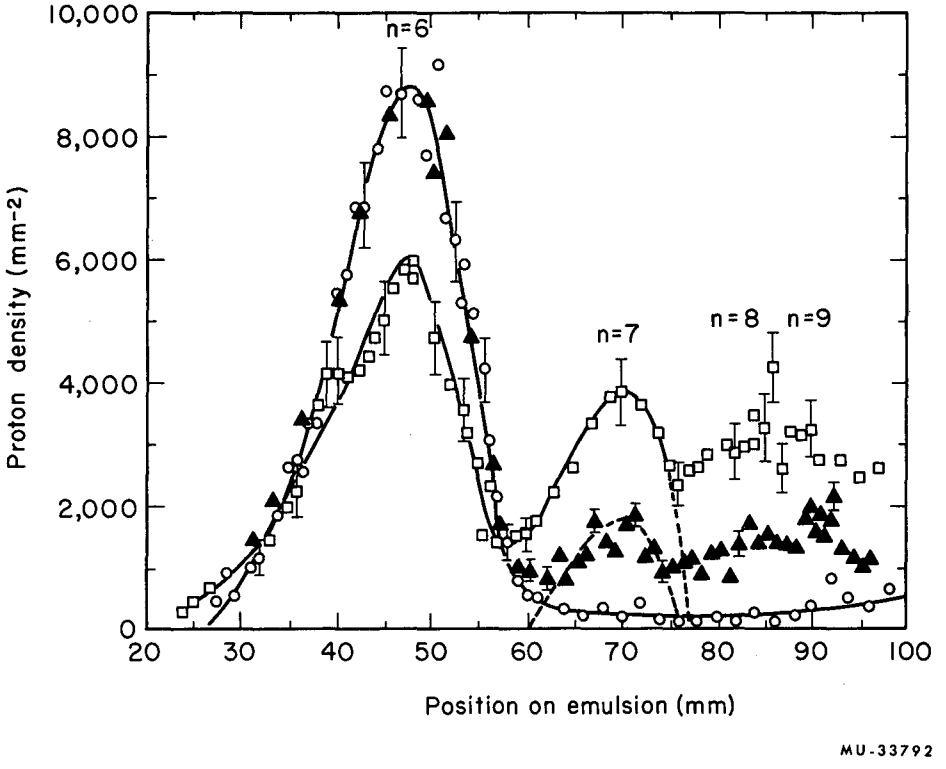

Fig. 18. Change in population of the levels n = 6 to 9 due to collisions with H_2. All levels above $n^* = 6$ of the incident beam were depopulated by Lorentz ionization in LM1. Pressure in target: 0, 5×10^{-5} torr (evacuated target); △ , 1.9×10^{-3} (low-density target) torr; □ , 0.1 torr (high-density target).

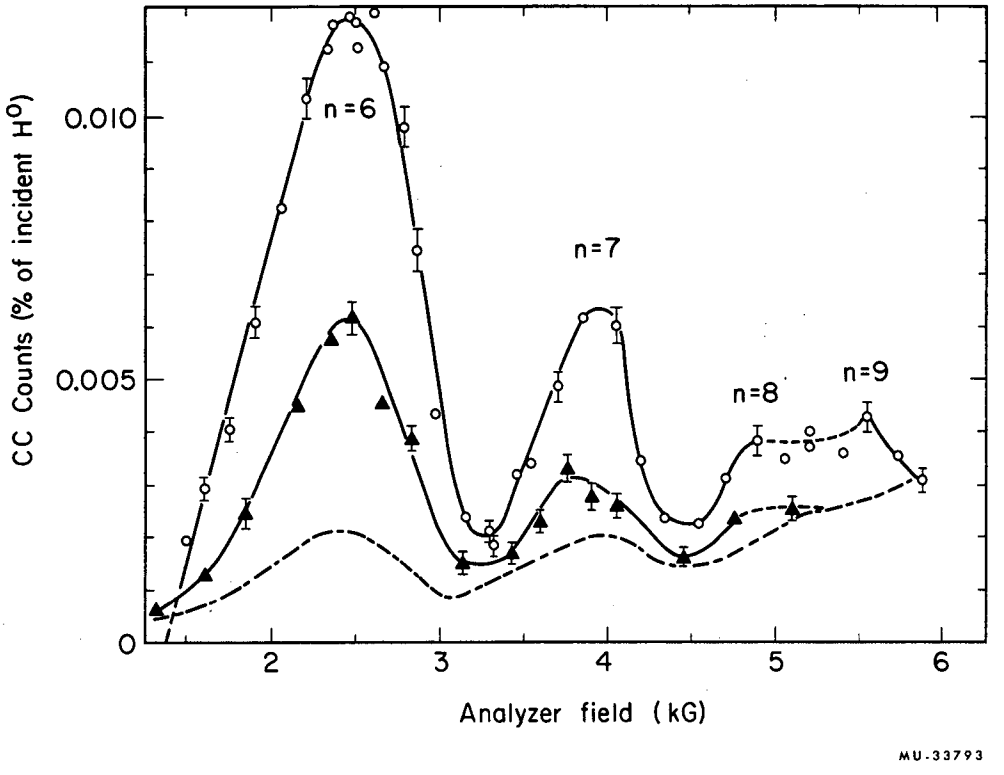

Fig. 19. Repopulation of the levels n = 6 to 9 due to collisions with charged particles. All levels above $n^* = 5$ of the incident beam had been depopulated by Lorentz ionization in LM1. The curve — - — is the result of collisions with neutrals (PIG off), which must be subtracted from the two upper curves to isolate the charged-particle effects. Only the applied voltage was changed to obtain different electron densities. The hydrogen-gas pressure was 3.0×10^{-3} torr; 0, $n_e = 2.2\times10^{12}$/cc; Δ, $n_e = 1.0\times10^{12}$/cc.

Table IV. Change in population of the levels n = 6 to 9, due to collisions with H_2, obtained by integrating the peaks of Fig. 18. All levels above $n^* = 6$ of the incident beam were depopulated by Lorentz ionization in LM1.

Pressure (10^{-3} torr)	Population of level n, N_n (% of total neutral beam)							
	Observed at LM2[a]				Corrected to target exit[b]			
	N_6	N_7	N_8	N_9	N_6	N_7	N_8	N_9
< 0.3	0.53	≈0.015	≈0.01	≈0.01	0.69	≈0.015	≈0.01	≈0.01
20	0.47	0.06	0.05	0.05	0.61	0.07	0.05	0.06
105	0.30	0.13	0.10	0.07	0.40	0.15	0.11	0.07

a. The experimental uncertainty is ±30% for N_6 and N_7 and ±40% for N_8 and N_9.

b. The observed populations were corrected for radiative decay (Fig. 25) to obtain the values at the target exit.

Table V. Change in population of the levels n = 6 to 9, due to collisions with charged particles in a hydrogen plasma, obtained by integrating the peaks of Fig. 19 and correcting for the effects of neutral collisions.

Target thickness, NL (10^{13} charged particles/cm^2)	Population of level n, N_n (% of total neutral beam)					
	Observed at LM2[a]			Corrected to target exit[b]		
	N_6	N_7	N_8+N_9	N_6	N_7	N_8+N_9
0	0	0	0	0	0	0
4.0	0.026	0.007	–	0.034	0.0075	–
9.3	0.069	0.017	0.011	0.089	0.022	0.012

a. The experimental uncertainty of these numbers is ±30%.

b. The observed populations were corrected for radiative decay (Fig. 25) to obtain the values at the target exit.

IV. ANALYSIS AND DISCUSSION

A. Qualitative Discussion of Changes in Excited-Level Population

The population of an excited state can be altered by Lorentz ionization, by radiative decay, and by inelastic collisions. All three processes are important in this experiment, but only one of the three is dominant in any particular region. Lorentz ionization of the excited states of interest in this experiment occurs only in two well-defined regions; in the first (LM1), the excited-state population is controlled before the beam enters the target, and in the second (LM2), the excited-state population of the beam emerging from the target is analyzed (see Fig. 5).

Radiative decay dominates in the long-evacuated drift sections of the experiment. Although the excited states under consideration have relatively long radiative lifetimes, appreciable depopulation occurs during the flight time to the detectors. We discuss this problem in Appendix F and present graphs showing the radiative decay of the levels n = 3 to 10. By means of Fig. 25 (Appendix F), the detected population can be corrected for radiative decay to give the population at the exit of the target chamber.

In the short, field-free target regions, inelastic collisions with the target particles dominate. Changes in excited-state population result from collision-induced excitation, de-excitation, ionization, and electron capture.

The plasma target, at first, seems rather complex since it contains ions, fast electrons, and neutrals. Several simplifications can be made, however. Of these, the separation of the effects of collisions with neutral particles from those with charged particles by pulsing the PIG only on every second beam pulse has already been discussed (Sec. III. C. 1).

The electron temperature in the PIG is of the order of 1 eV (Fig. 10), which corresponds to a thermal velocity of the order of

5×10^7 cm/sec. Comparing this with the incident H^0 velocity of 4.37×10^9 cm/sec, we can conclude that the electrons in the plasma can be considered to be at rest with respect to the beam. The few energetic electrons from the tail of the Maxwell distribution, or the few runaway electrons observed in low-pressure PIG discharges, which might have velocities greater than that of the incoming beam, should not noticeably affect cross-section measurements. At these velocities, the cross section varies approximately inversely with the kinetic energy of relative motion, and these few fast particles will go essentially unnoticed.

Another simplification resulting from the use of a 10-MeV beam is that electrons and protons have the same cross sections for collisional excitation and ionization. In the first Born approximation, the cross sections for inelastic collisions of H atoms with charged particles depend only on the relative velocity of the charged particle with respect to the atom, not on the mass.[12, 13, 16, 50] At low energies, the FBA is not valid, and the above statement does not hold. This equivalence at high energies has been demonstrated by Hooper et al. for ionization of several gases by electron and proton impact.[51] The cross sections were found to be equivalent, within experimental error, for incident velocities greater than 1×10^9 cm/sec. Ionization is only a limiting case of excitation, namely excitation into the continuum; since the FBA predictions have been verified by Hooper et al. for this limiting case, we can assume the more general FBA prediction with some confidence. Consequently, our plasma will be treated as a stationary target of a single species of charged particles.

B. Quantitative Description of Changes in Excited-Level Population

1. Coupled Equations for e-H Collisions

A complete description of the changes in the population of the excited levels as the H^0 beam passes through the target requires a knowledge of the excitation, ionization, and production cross sections

for all levels. For e-H collisions, many of the cross sections have been calculated (Sec. II), and it is possible to predict the changes in population resulting from these collisions. No such analysis can be made for collisions with H_2 since the cross sections have not been calculated.

For e-H collisions, the calculated excitation cross sections $\sigma_{n,n'}$ are relatively small except when $\Delta n = n' - n = \pm 1$ (Table I). Furthermore, at 10 MeV the cross section for electron capture by protons is very much smaller than excitation or ionization cross sections[52] and may be neglected. We can also neglect radiative decay in the target because of the long lifetimes of the levels of interest (Appendix F).

The change in population of the level n due to e-H collisions can therefore be described by the relation

$$\frac{dN_n}{d\pi} = - N_n(\pi)\,(\sigma_{n,C} + \sigma_{n,n-1} + \sigma_{n,n+1}) + N_{n-1}(\pi)\,\sigma_{n-1,n} + N_{n+1}(\pi)\,\sigma_{n+1,n} \qquad (11)$$

where π is the number of electrons per cm^2 traversed by the beam (distance times target density), and $N_n(\pi)$ is the number of atoms in the level n after passing through an element of target thickness π. The first term on the right-hand side describes the losses from the level n due to ionization, excitation, and de-excitation of that level. The second and third terms describe gains resulting from excitation and de-excitation of the neighboring levels.

We now have an infinite set of coupled differential equations, which we must truncate if we hope to get a solution. We have somewhat arbitrarily chosen to truncate these equations at $n = 10$. This was governed by two practical considerations. The first was an experimental one. We can determine only the population of $n = 6$ to 9, and higher levels are of interest only insofar as they affect the population

of these levels. Our method of preparing the beam is such that the levels with $n > 10$ are completely depopulated by Lorentz ionization before they strike the target. The only way that these levels can influence the lower ones is by a secondary de-excitation following an excitation of one of these levels; however, the second collision has a 20% larger probability for excitation to still higher levels than de-excitation (see Table I). We therefore treated all levels above $n = 10$ as sinks.

The second reason for this particular truncation was the availability of cross-section data. At the time that these equations were programmed, the only available excitation cross sections were those of Milford and co-workers,[19-24] who had calculated them up to $n = 10$.

The solution of the Eq. (11) is discussed in Sec. V. C. 1.

2. The Thin-Target Approximation

For thin targets, in which a collision mean-free path is large compared to the length of the target (i. e., $\sigma << \Pi^{-1}$, where Π is the total target thickness), we can assume that none of the H atoms undergoes more than one collision. For this case, consider an incident beam of H atoms that has been prepared in such a way that none of the levels above a given n, designated n^*, are populated. If the excitation cross section σ_{n^*, n^*+1} dominates over σ_{n^*, n^*+2}, σ_{n^*, n^*+3}, $\cdots$, then the growth in the population of the $n^* + 1$ level will be given by

$$\frac{dN_{n^*+1}}{d\pi} \approx N_{n^*}(\pi)\, \sigma_{n^*, n^*+1} \cdot \tag{12}$$

Furthermore, the value of N_{n^*} will not change appreciably in a thin target, and we get the approximate solution

$$\sigma_{n^*, n^*+1} \approx \frac{1}{\Delta\Pi} \frac{\Delta N_{n^*+1}(\Pi)}{N_{n^*}(\Pi = 0)} \cdot \tag{13}$$

For collisions with H_2, the repopulation of the levels $n^* + 2$, $n^* + 3$, $\cdots$ is comparable to that of the level $n^* + 1$, yet all change in proportion to Π (Table IV and Fig. 18). This indicates that transitions with $\Delta n > 1$ are contributing significantly to the changes in population. For this case there is no simple solution, even in the thin-target limit. We can, however, obtain an upper limit for the cross section $\sigma_{n^*,\, n^*+1}$ from Eq. (13) and for $\sigma_{n^*,\, n^*+2}$, etc., from similar equations.

V. EXPERIMENTAL RESULTS

A. Lorentz Ionization

The threshold fields for Lorentz ionization of the levels n = 5 to 9 were measured by observing the decrease in the population of these levels as the field in the first stripping magnet, LM1, was gradually increased. The target was evacuated so that no collisional repopulation occurred. The results are shown in Fig. 20. The abscissa is given in terms of the equivalent electric field ($\underset{\sim}{F} = \underset{\sim}{v} \times \underset{\sim}{B}$ = 43.7 kV/cm/kG) produced by LM1. Also shown is the range of electric field for which ionization of the particular level should occur in 2×10^{-10} sec, according to the Rice and Good calculations (Fig. 2).[6,7] The n = 5 curve (Fig. 20) is indicated by a dashed line because the field of LM2 could not be raised high enough to ionize all the states of the level n = 5. The rapid attenuation of each level, as the magnetic field of LM1 was raised slightly above the threshold field, is consistent with a statistical distribution of the population of the states within each quantum level (see Fig. 3).

B. Population of Excited Levels of Hydrogen Atoms Formed by Collisional Dissociation of H_2^+

The population of the levels n = 6 to 9 of hydrogen atoms formed by the collisional dissociation of H_2^+ [Eq. (10)] in H_2 was obtained by integrating the Lorentz ionization profile of Fig. 13. The results are shown in column 2 of Table VI. These were corrected for radiative decay (Fig. 25) to give the population at the exit of the first gas cell (column 3). The neutral beam produced by H_2^+ dissociation is expected[45,46] to have excited populations produced in proportion to A/n^3; A can range from 2 to 8, depending on the vibrational population of the H_2^+. From Table VI we see that the observed populations are in agreement with A/n^3 distribution, and for the H_2^+ beam used in this experiment, $A \approx 3$.

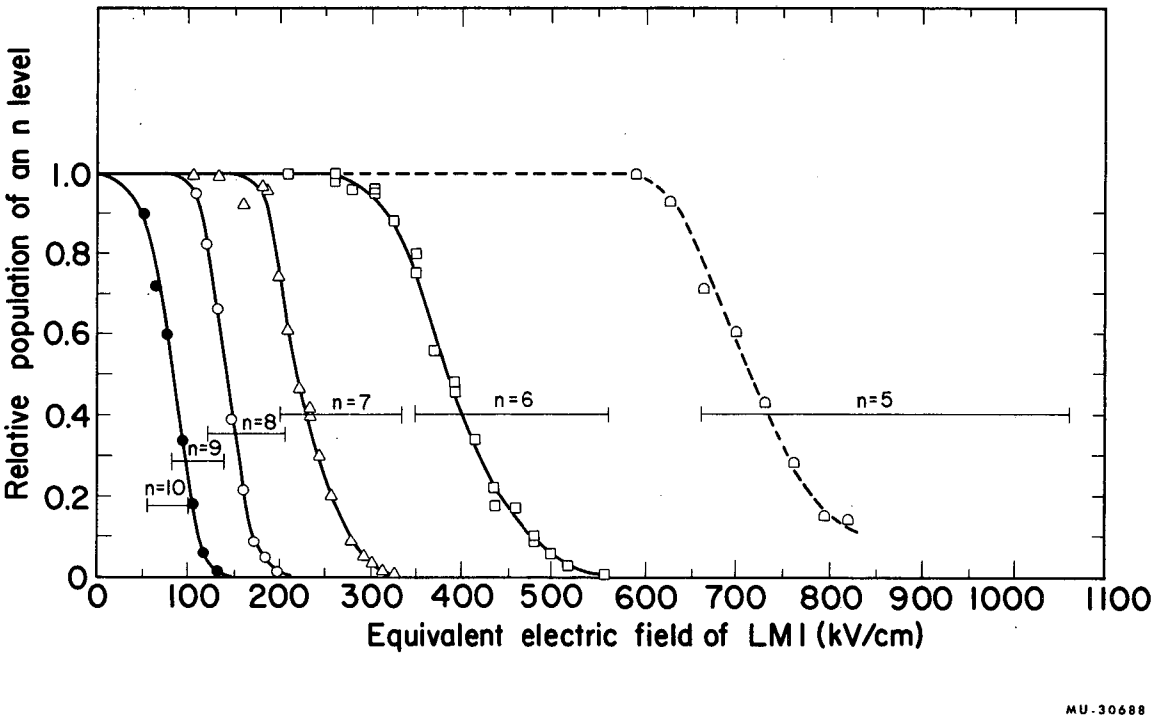

Fig. 20. Decrease in the population of excited levels as a function of the equivalent electric field (F = 43.7 kV/cm per kG) of the first stripping magnet LM1. Also shown for each level is the predicted range of electric field corresponding to a mean life of 2×10^{-10} (see Fig. 2). For explanation of dashed line, see text.

Table VI. Population (% of H^0 beam) of the levels n = 6 to 9 of atomic hydrogen formed by collisional dissociation of H_2^+ on H_2 (from the experimental data of Fig. 13). See errata on this

n	Experimental populations	Experimental populations corrected for decay (in 450 cm)	$2/n^3$	$3/n^3$	$\frac{\text{nth level}}{\text{(n + 1)th level}}$ Experimental populations corrected for decay	$\frac{\text{nth level}}{\text{(n+1)th level}}$
6	0.65±0.20	1.09	0.92	1.38	1.16	1.59
7	0.72±0.21	0.94	0.58	0.87	1.54	1.49
8	0.52±0.21	0.61	0.39	0.58	1.56	1.42
9	0.35±0.14	0.39	0.27	0.40		

The target thickness, $\Pi = 2.0\times10^{-16}$ molecules/cm^2, was relatively thin for excitation (Sec. V. C. 2), and it is unlikely that the population was modifed by excitation collisions. In a separate experiment, we measured the cross section for the reaction

$$H_2^+ + H_2 \rightarrow \sum_n H(n) + H^+ + H_2 , \qquad (14)$$

and found it to be $\sigma = 1.6\times10^{-18}$ cm^2/molecule.[85] Using this and assuming that the $3/n^3$ distribution can be extrapolated to all levels $n > 1$, we obtain for the reaction

$$H_2^+ + H_2 \rightarrow H(n) + H^+ + H_2 \qquad (15)$$

the cross sections:

$$\sigma[H_2^+ \rightarrow H(1)] \approx 0.64\times10^{-18} \text{ cm}^2/\text{molecule}$$

for $n = 1$, and

$$\sigma[H_2^+ \rightarrow H(n)] \approx 1.9\times10^{-18} \text{ cm}^2/\text{molecule}$$

for $n > 1$.) see errata on this.

C. Excitation Cross Sections

1. Plasma Target

a. Thin-target approximation results.

The experimental results for excitation by charged particles in a hydrogen plasma, analyzed in the thin-target approximation, are given in Table VII. For these calculations, the observed population of each level was corrected for radiative decay (Fig. 25) occurring in the 225-cm drift section between the target exit and LM2. Additional assumptions that had to be made are noted in the table. Also listed in Table VII are the corresponding theoretical Bethe or FBA cross sections for e-H collisions (Table I).

Table VII. Cross sections $\sigma_{n,\,n'}$ for excitation of 10-MeV H atoms by collisions with charged particles in hydrogen plasma (10^{-18} cm^2/charged particle). The experimental uncertainty is ±40% for the absolute values and ±25% for the relative values (see Sec. V. E. 2).

	Experimental[a]					Theoretical[b]		
n \ n'	6	7	8	9	8+9	6	7	8
1	< 1.3[c]	< 0.5[c]				0.058	0.035	
4	< 98[c, d]	< 38[c, d]				43		
5	630[d]	140[d]			90[e]	846	93	
6		1700	510	190			1650	175

a. The experimental results analyzed in the thin-target approximation.

b. The corresponding numbers from Table I for e-H collisions are repeated here for comparison.

c. The n = 2 and 3 levels were almost completely depopulated by radiative decay in the 2-meter drift section (Fig. 25). Therefore, when LM1 was set to Lorentz ionize n > 4, the observed repopulation could be due only to excitation from n = 1 or 4. The numbers are upper limits for each of these processes.

d. Since LM2 could not determine the population of n < 6, we assumed a $3/n^3$ distribution (Sec. V. B) corrected for radiative decay: $N_5/N_1 = 0.014$ and $N_4/N_1 = 0.013$.

e. Although n = 8 and 9 could not be resolved, the combined population could be determined.

We see that the cross sections for transitions with $\Delta n = 1$ dominate. We find good agreement with theoretical calculations except that the $\Delta n = 2$ transitions are slightly larger than calculated.

b. Solution to the coupled equations.

By use of the theoretical cross sections of Sec. II and with the assumption of an initial population given by $3/n^3$ corrected for radiative decay (Sec. V. B), the Eqs. (11), and similar equations including n to (n + 2) transitions, were solved on an IBM 7044 computer. The predicted populations of the levels n = 6 to 9 are shown in Figs. 21 to 23 for $n^* = 5$. The points on the curves are the observed populations corrected for radiative decay. These changes in population occurred for atoms whose states are Stark split by the Lorentz-transformed magnetic field of the earth (see Appendix F). They should, therefore, be compared with solutions to the Eqs. (11) for cross sections connecting Stark states, whereas the only available cross sections have been calculated for the field-free case (Sec. II). In Appendix G we justify the use of theoretical, field-free calculations for comparison with the experimental results.

Figures 21 to 23 illustrate the relatively large contribution of $\Delta n = 2$ transitions to the repopulation of these levels, even though the cross sections $\sigma_{n,\, n+2}$ are about a tenth as big as $\sigma_{n,\, n+1}$ (Table I). The repopulation of n = 6 (Fig. 21) is in good agreement with the theoretical prediction. The growth in the population of n = 7, however, is larger than the theoretical prediction (Fig. 22). This is consistent with our thin-target approximation result (Table VII) that the cross section $\sigma_{5,\,7}$ is somewhat larger than the theoretical value.

Figure 23 shows that the theoretical predictions based on $\Delta n = 1$ and 2 transitions considerably underestimate the observed repopulation of the levels n = 8 and 9. Our thin-target results indicate that $\sigma_{5,\,8+9} \approx 1/2\, \sigma_{5,\,7}$ (Table VII), and this value for a $\Delta n = 3$ transition would explain the observed repopulation of $N_8 + N_9$.

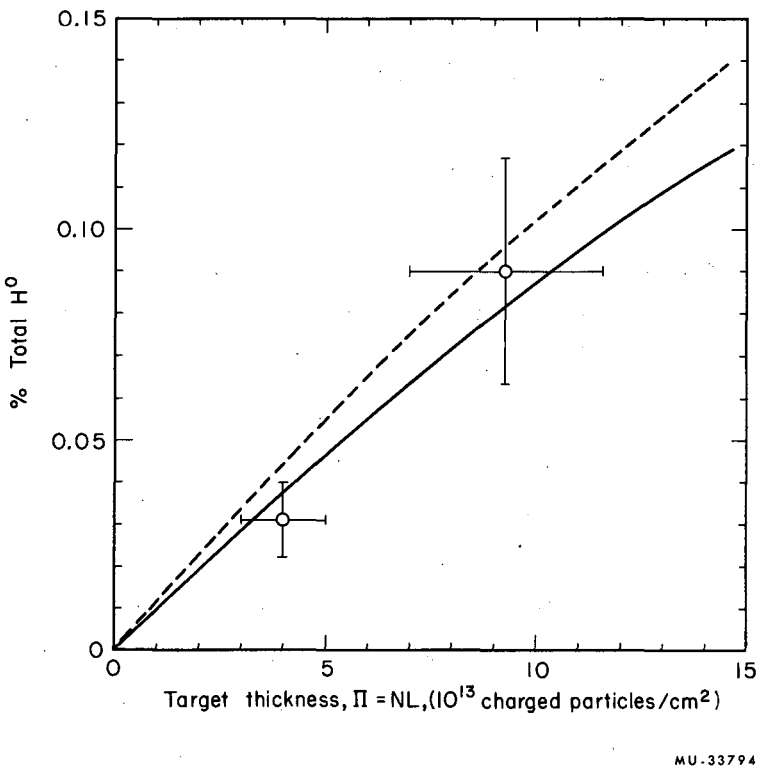

Fig. 21. Repopulation of the level n = 6 due to collisions with charged particles in a hydrogen plasma for the case $n^* = 5$. The dashed line is the solution to the Eqs. (11), which include the effects of ionization and $\Delta n = 1$ excitation and de-excitation. The solid line is the solution to similar equations in which $\Delta n = 2$ transitions have also been included. Both of these results are based on theoretical excitation (Table I) and ionization (Table III) cross sections. The points represent experimental results.

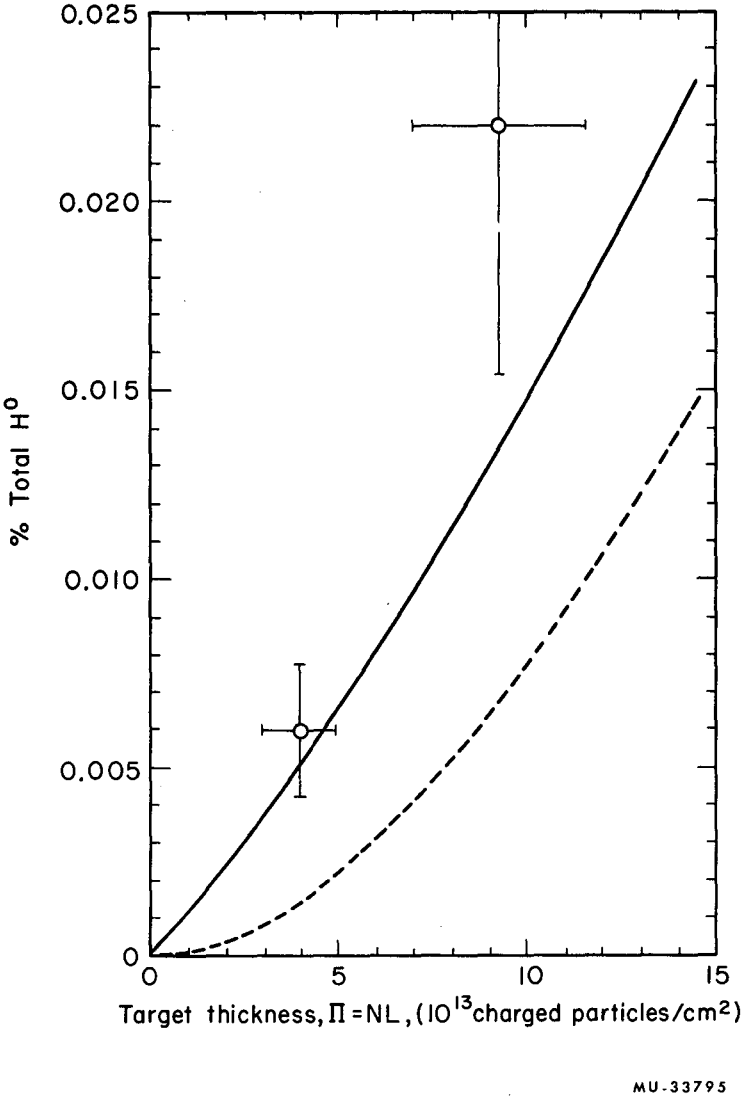

Fig. 22. Repopulation of the level n = 7 due to collisions with charged particles in a hydrogen plasma for the case $n^* = 5$. Symbology is the same as in Fig. 21.

See errata on this

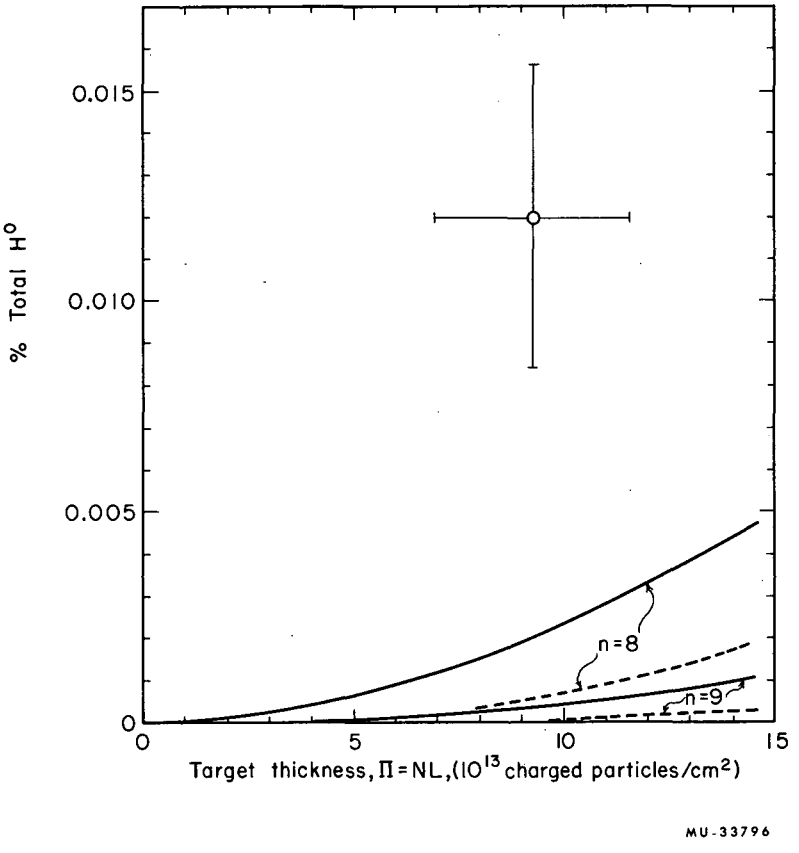

Fig. 23. Repopulation of the levels n = 8 and 9 due to collisions with charged particles in a hydrogen plasma for the case $n^* = 5$. Symbology is the same as in Fig. 21.

2. $H\text{-}H_2$ Collision Cross Sections

The experimental results for excitation from all levels $n \leq 4, 5, 6$ to the levels $n' = 6, 7, 8,$ and 9 are presented in Table VIII.

The observed repopulation of the levels n = 6 to 9 indicated that transitions with $\Delta n > 1$ are comparable to those with $\Delta n = 1$ for collisions with H_2. Consequently, a thin-target analysis can determine only upper limits for the cross sections for the individual transitions from $n = 1, 4, 5, 6$ to $n' = 6, 7, 8, 9$. These are shown in Table IX.

Comparing these $H\text{-}H_2$ cross sections with those for excitation by a fully ionized plasma (Table VII) we note several distinct differences: (a) The $H\text{-}H_2$ cross sections are at least two orders of magnitude smaller; (b) they do not vary appreciably with n; and (c) the transitions with $\Delta n > 1$ are comparable to those with $\Delta n = 1$ and decrease very slowly with increasing Δn.

At high energies, the observed cross sections for ionizing collisions with molecular hydrogen agree with theoretical calculations for collisions with atomic hydrogen.[15] This suggests that we may compare the results of Table IX with the FBA results of BHM (Table II), which give lower limits for the H-H collision cross sections for the levels n = 2 to 4. The observed weak-n dependence is consistent with the BHM calculations; however, a rough extrapolation of these results to higher n values yields magnitudes smaller than the measured values. Although our results are only upper limits, they suggest that the other processes (5) and (6) discussed in Sec. II. B. 2, may contribute significantly to the excitation process. The fact that transitions with $\Delta n > 1$ are comparable to those with $\Delta n = 1$ is consistent with the FBA results of Bates and Griffing[16] for H(1s)-H(1s) collisions.

Table VIII. Cross sections for excitation from all levels $n \leq 4, 5, 6$ to levels $n' = 6, 7, 8,$ and 9 for collisions with H_2 (10^{-18} cm^2/molecule). The experimental uncertainties in the absolute values are ±30% for the columns $n' = 6$ and 7 and ±40% for $n' = 8$ and 9; the relative uncertainties are ±20% and 30% respectively (see Sec. V. E. 3).

	$n'=6$	$n'=7$	$n'=8$	$n'=9$
$n \leq 4$	0.013	0.011	0.0092	0.0066
$n \leq 5$	0.019	0.014	0.012	0.0053
$n \leq 6$		0.028	0.019	0.016

Table IX. Upper limits for the cross sections $\sigma_{n,\,n'}$ for excitation by collisions with H_2 (10^{-18} cm^2/molecule).[a]

n \ n'	6	7	8	9
1	0.013	0.011	0.009	0.007
4	1.0[b]	0.8[b]	0.7[b]	0.5[b]
5	1.4[b]	1.0[b]	0.8[b]	0.4[b]
6		5.3	3.5	2.8

a. Experimental results analyzed in thin-target approximation.

b. Since LM2 could not determine the population of $n < 6$, we assumed a $3/n^3$ distribution (Sec. V. B) corrected for radiative decay: $N_5/N_1 = 0.014$ and $N_4/N_1 = 0.013$.

D. Ionization Cross Sections

No quantitative results could be obtained for the ionization cross sections $\sigma_{n,C}$. However, for either target the depletion in the population of the level n^* could always be explained by the observed repopulation of the higher levels. This suggests that the ionization cross sections for these levels are smaller than the excitation cross sections, which is consistent with the calculations for e-H collisions (Table III).

E. Experimental Uncertainties

1. Population of the Levels n = 6 to 9

The population measurements for the levels n = 6 and 7 were reproducible within 15% when measured with the counters and within 20% when measured with emulsions. However, the emulsion measurements were typically 20 to 30% lower than the counter measurements. We therefore assign an uncertainty of ±30% to the absolute values of these measurements.

The levels n = 8 and 9 were usually not well resolved, and we assign an uncertainty of ±40% to the individual measurements and ±30% to the sum of $N_8 + N_9$.

2. Excitation Cross Sections for the Fully Ionized Hydrogen Plasma

The absolute uncertainty in the electron density is believed to be ±25% (Sec. III. B. 2); combining this with the uncertainties in populations we obtain an uncertainty in the absolute values of Table VII of ±40% and a relative uncertainty of ±25%. Those cross sections which require an assumption about the initial population of N_4 or N_5 (superscript d) have the same relative uncertainty, but the absolute uncertainty is unknown.

3. Excitation Cross Sections for $H-H_2$ Collisions

The uncertainty in the absolute pressure was taken to be ±10%. The uncertainty in the absolute values of the cross sections listed in Tables VIII and IX is therefore ±30% for columns $n' = 6$ and 7 and ±40% for $n' = 8$ and 9; the relative uncertainties are ±20% and ±30%, respectively. Again, those cross sections that require an assumption about the initial population of N_4 or N_5 (superscript b) have the same relative uncertainty, but the absolute uncertainty is unknown.

VI. SUMMARY AND CONCLUSIONS

We have found that the electric-field ionization thresholds for the levels n = 5 to 9 predicted by the Rice and Good model are in good agreement with the observed Lorentz ionization of 10-MeV hydrogen atoms. It was not possible, however, to resolve the thresholds for ionization of individual states of a level in this experiment. Lorentz ionization enabled us to depopulate all levels above a predetermined value $n^* > 4$, and to observe the repopulation of the levels n = 6 to 9 due to collisional excitation in a target.

The population distribution over excited levels of hydrogen atoms produced by collisional dissociation of H_2^+ on H_2 was found to be $N_n/N_1 \approx 3/n^3$ for n = 6 to 9. This is consistent with estimates by Hiskes.

The results for collisional excitation of 10-MeV H atoms by charged particles are in good agreement with theoretical predictions in the first Born approximation. Agreement of experimental results with the FBA at high energies has long been established for collisions that require a large momentum transfer (excitation or ionization from the ground state). The validity of the FBA has now been established for the small momentum transfer required for the collisions studied in this experiment. The problem of determining the low-energy limit for agreement between experiment and FBA calculations is yet unsolved. The Lorentz ionization technique can be used at lower energies, but stronger magnetic fields will be required.

The cross sections for excitation from the levels $n \leq 4, 5, 6$ to the levels n = 6 to 9 have been measured for H-H_2 collisions. From these measurements upper limits for the cross sections of the individual transitions from n = 1, 4, 5, 6 to n' = 6 to 9 have been obtained. These cross sections are of the order of 10^{-18} cm^2/molecule, at least two orders of magnitude smaller than those for collisions with charged particles in a hydrogen plasma. Unlike the charged-particle cross sections, they are weakly dependent on n and collision-induced transitions with $\Delta n > 1$ are comparable to those with $\Delta n = 1$. Although no quantitative measurements of the ionization cross sections could

be made, the experimental results in both targets indicate that they are small compared to the excitation cross sections for the levels n = 6 to 9. This is consistent with Bethe calculations for e-H collisions.

ACKNOWLEDGMENTS

I wish to thank Dr. Robert V. Pyle for his active interest and supervision, and Dr. C. M. Van Atta for his support of this research. Also: Dr. John R. Hiskes for many valuable discussions on the theoretical aspects of the problem; Dr. Selig N. Kaplan and Dr. George A. Paulikas for their participation in the experiments; J. Warren Stearns and Vincent J. Honey for their help in the construction and operation of the equipment; Donald B. Hopkins for conducting the microwave diagnostics; Carl Quong for programming the computer solutions; and Margaret R. Thomas for her patience in typing the preliminary draft of the manuscript.

Figures 2 and 3 are from UCRL-7582 by John R. Hiskes and David S. Bailey; their permission to use these curves prior to publication is gratefully acknowledged.

This work was performed under the auspices of the U. S. Atomic Energy Commission.

APPENDICES

A. A Brief Survey of the Available Cross Sections for Inelastic Collisions of Hydrogen Atoms with Electrons, Protons, or Other Hydrogen Atoms

Work on inelastic collisions of hydrogen atoms with electrons, protons, or other hydrogen atoms has been reviewed by Mott and Massey,[12] Massey and Burhop,[13] and, more recently, by Seaton,[14] Fite,[15] Bates,[16] Heddle and Seaton,[17] and Milford.[18]

1. e-H Collisions

Measurements for excitation cross sections by electron impact have been reported for the transitions 1s-2s, 1s-2p, and 1s-3. The cross section for 1s-2p excitation has been measured by Fite and Brackmann[53] and by Fite et al.[54] In these experiments relative measurements were obtained by observing the collisionally induced Lyman-α radiation; absolute values were obtained by normalizing these results to Born approximation calculations at 250 eV. The 1s-2s excitation cross section has been measured by Lichten and Schultz,[55] who detected metastable 2s atoms with a platinum surface, and by Stebbings et al.,[56] who measured the Lyman-α radiation from electrically perturbed 2s metastables. Apparent conflicts in the original results of the two experiments have since been resolved.[57,58] Recently Kleinpoppen et al., reported collisional excitation of the Balmer-α line for electron energies from 20 to 100 eV, giving the cross section for excitation from n = 1 to 3.[59]

Theoretical calculations for excitation of hydrogen atoms by electron impact are more numerous than experimental results. First Born approximation (FBA) calculations for the transitions 1s-2s, 2p, 3s, 3p, 3d, and 2p-3s, 3p, 3d are tabulated in Massey and Burhop for electron energies from 20 to 1000 eV.[60] McCarroll has calculated FBA cross sections for excitation from the ground state to n = 2, 3, 4 and has used an extrapolation technique to calculate the cross sections

for excitation to all other levels.[36] This technique has also been applied to excitation from 2s[37] and 2p[38] to all higher levels.

Calculations for the 1s-2s and 1s-2p transitions have also been carried out in higher approximations (second Born, distorted wave, exchange effects, etc.).[14, 17, 61-69] The results of all these methods converge and agree with the previously mentioned experiments above 200 eV. At lower energies, however, the results vary and are typically twice as big as those obtained experimentally. For the lower energies Akerib and Borowitz[70] have used an impulse approximation, and Seaton[34] has used a semiclassical impact-parameter method; these results are in better agreement with those obtained experimentally.

For higher n values there are the recent results of Milford and co-workers,[19-24] who have calculated cross sections for collisions in which $\Delta n = +1$, or $+2$ and $\Delta \ell = +1$ for $n = 1$ to 10. These are carried out partly in the first Born and partly in the Bethe approximation. The results are summarized in the last paper.[24]

The FBA results indicate that e-H excitation cross sections increase rapidly with increasing n (approximately as n^4) and that collisions with $\Delta n = 1$, $\Delta \ell = 1$ dominate over all other modes of excitation.

Ionization of H(1s) by electron impact has been investigated experimentally[15, 41] and theoreticaly.[12, 14, 42, 70, 71] Ionization cross sections for higher n values have been calculated only theoretically.[38-40, 43, 44, 72] For the ground state, ionization cross sections are comparable to $n = 1$ to 2 excitation. For $n > 3$ the ionization cross sections seem to increase almost linearly with n at the higher energies.[39] Since excitation cross sections increase more rapidly with n, theoretical results indicate that excitation dominates over ionization for large n values.

2. p-H Collisions

Cross sections for collisional excitation by proton impact have been calculated in the FBA for 1s-2s, 2p, 3s, 3p, and 3d transitions,[16] and for some transitions of excited states up to n = 10.[73] The 1s-2s, and 2p transitions have also been calculated in higher approximations.[16,63,74-76] At high energies the FBA gives the same results for impact by electrons as for protons of the same velocity;[12, 13, 16, 50] consequently, at high energies the calculations of Milford and co-workers[24] may be used. No experimental results for excitation by proton impact have been reported.

3. H-H Collisions

Excitation cross sections for atom-atom collisions have been calculated in the FBA for collisions of the type

$$H(1s) + H(1s) \rightarrow H(1s) + H(2s \text{ or } 2p) \qquad (A-1)$$

$$\rightarrow H(2s \text{ or } 2p) + H(n, \ell) \qquad (A-2)$$

for $n\ell$ = 2s, 2p, 3s, 3p, 3d, continuum,[16] and for collisions of the type

$$H(n\ell) + H(1s) \rightarrow H(n', \ell') + H(2s) \qquad (A-3)$$

$$\rightarrow H(n', \ell') + H(2p) \qquad (A-4)$$

for n = 2, 3, 4, and $n' = n + 1$.[25] The results indicate that at high energies the excitation cross sections for atom impact are two or more orders of magnitude smaller than the corresponding proton impact cross sections.[50]

Experimental results have been reported only for molecular hydrogen targets. Ionization by collisions with H_2 has been measured for H(1s)[49,52] and H(n = 14).[77] Preliminary results of the present experiment have been reported for excitation from n = 6 to 7 by collisions with H_2.[11]

B. On the Equivalence of Electric Field and Lorentz Ionization for 10-MeV Hydrogen

Although ionization by electric fields has been treated in detail, no calculations have been carried out for the problem of an atom moving through a magnetic field. Hiskes[26] has shown that by introducing the Lorentz field, $\underset{\sim}{F} = \underset{\sim}{v} \times \underset{\sim}{B}$, the two problems are identical except for the Zeeman terms, but the effect of these terms has not been determined. For high velocities and magnetic fields of the order of 10 kG, Zeeman splitting is small compared to Stark splitting, and no gross effects are expected.

This is readily seen by comparing extreme values for the two effects. For high magnetic fields the Zeeman shift in energy is given by $\Delta W = B\mu_0(m_\ell + 2m_s)$, where μ_0 is the Bohr magneton. The maximum value of this shift will occur for the largest value of m_ℓ, namely $m_\ell = n - 1$. The appropriate magnetic field ($B = F/v$) to use is that which will give a Lorentz electric field strong eough to ionize the state under consideration in the time that the atom is in the magnetic field. For an upper limit we will use the maximum field required to achieve the experimentally imposed ionization rate for each level n (Fig. 2). The maximum Zeeman splitting will then be given by

$$(\Delta W)_{max} \approx \frac{2\mu_0 n F_{max}}{v} \approx 0.26\times 10^{-6}\, n F_{max}\ (kV/cm) \qquad (B\text{-}1)$$

electron volts for 10-MeV hydrogen atoms ($v = 4.37\times 10^9$ cm/sec). The values of F_{max} and the corresponding $(\Delta W)_{max}$ are given in Table B-I for the levels n = 5 to 9.

A lower limit for the energy difference between neighboring Stark states ($n_1 - n_2 = 1$) is the spacing obtained for the linear Stark effect,[30]

$$(\Delta W)_{min} = 1.5\, n\, F(a.u.) \approx 8\times 10^{-6}\, n\, F_{min}\ (kV/cm) \qquad (B\text{-}2)$$

Table B-I. Comparison of maximum Zeeman splitting and minimum Stark state separation for 10-MeV hydrogen atoms.

n	F_{max}	F_{min}	Zeeman split $(\Delta W)_{max}$	Stark separation $(\Delta W)_{min}$
	kV/cm		Electron Volts	
5	1100	680	0.0015	0.03
6	570	350	0.0009	0.02
7	340	220	0.0006	0.01
8	200	120	0.0004	0.01
9	140	80	0.0003	0.006

electron volts. Here F_{min} is the minimum field required to achieve the experimentally imposed ionization rate for each level (Fig. 2). F_{min} and $(\Delta W)_{min}$ are also shown in Table B-I.

Comparing the two limiting cases listed in the table, we see that at this velocity the Zeeman splitting is always much smaller than the spacing between Stark states for the levels considered. Therefore, we expect no difference between Lorentz and electric field ionization for 10-MeV hydrogen atoms.

This calculation, based on a rough upper limit for the Zeeman splitting and a rough lower limit for the Stark splitting, cannot predict the energy at which one might expect to observe a difference between electric field and Lorentz ionization. Experimentally no difference has been observed by Riviere and Sweetman for 50-keV H atoms.[9] Since this experiment could not resolve the ionization thresholds for the individual states of a level n, and since the atoms did not spend equal times in the electric- and magnetic-field regions, no precise measurements could be made.

C. Discussion of the Construction of Table I

To obtain the effective cross sections connecting various levels, a statistical distribution over states was assumed, and the results of Fig. 4 were averaged according to

$$\sigma_{n,\,n'} = \frac{1}{n^2} \sum_{\ell=0}^{n-1} (2\ell + 1)\ \sigma(n,\ \ell \rightarrow n'\ell + 1)\ . \qquad \text{(C-1)}$$

These are the entries with superscript a in Table I.

The results of Seaton's semiclassical impact parameter method[34] are labeled with superscript b. These numbers are statistical averages for the n to n + 1 transitions for which $\Delta\ell = 1$.[35]

The entries with superscript c are the FBA results for $\sigma_{1,\,n}$ of McCarroll.[36] The published results were tabulated for electron energies up to 1 keV, and evaluation of the analytic expressions at higher energies would have involved much calculation. The cross sections $\sigma_{1,\,n'}$ plotted as a function of energy over the range 100 to 1000 eV, produced a straight line for each n on log-log paper. These straight lines, which indicated an $E^{-0.8}$ energy dependence, were extrapolated to 5425 eV to obtain the values entered in Table I. The entries are bracketed to warn the reader that an extrapolation was used.

The cross sections entered in Table I with superscript d were obtained by averaging the FBA results of McCrea and McKirgan[37] for $\sigma(2pm \rightarrow n)$ and the results of Boyd[38] for $\sigma(2s \rightarrow n)$ over substates. For this, we used the relation

$$\sigma_{2,\,n} = \frac{1}{4}\left\{\sigma(2s \rightarrow n) + \sum_{m=-1}^{1} \sigma(2pm \rightarrow n)\right\}. \qquad \text{(C-2)}$$

We then took the averaged results and extrapolated them to our energy of 5425 eV, using the method described previously. Again the cross sections were found to have an energy dependence $\approx E^{-0.8}$. The published results were tabulated only up to 120 eV, and the extrapolation to almost fifty times that energy is difficult to justify. However, for $n' = 3$ and 4 these entries can be compared with unextrapolated FBA results. This comparison indicates that these values (denoted by superscript d) may be high by a factor of two. Again the entries are bracketed to remind the reader that these are extrapolated results.

The results $\sigma_{n,\,n'}$ for $n < n'$ were obtained by using the relation

$$\sigma_{n',\,n} = \left(\frac{n'}{n}\right)^2 \sigma_{n,\,n'}\,, \qquad \text{(C-3)}$$

which is discussed in Sec. II. B. 3.

It is interesting to note that many of these cross sections for electron impact can be approximated at high energies by an $E^{-0.8}$ energy dependence. This weak energy dependence is a result of the $E^{-1}\ \ell n\ E$ form that is typical for electron collisions that cause optically allowed transitions (nonvanishing dipole matrix element).[12, 16] Atom-atom collisions, on the other hand, seem to have an asymptotic energy dependence of E^{-1}.[16, 25]

D. The Relationship between Excitation and De-excitation Cross Sections

The general relation between collisional excitation and de-excitation cross sections can be derived from the principle of microscopic reversibility.[78] In this experiment we are interested only in the relation at high relative velocities. Here the relation can be established readily from consideration of the first Born approximation.

In the FBA, the cross section for a transition from an initial state p to a final state q is given by Eq. (1). In the FBA, $\langle p|V|q\rangle = \langle q|V|p\rangle$, and we get the relation

$$v_p^{\,2}\,\sigma(p \to q) = v_q^{\,2}\,\sigma(q \to p)\ . \qquad \text{(D-1)}$$

Let us now consider the excitation of a hydrogen atom. Let the atom be in the states n, ℓ, m and n', ℓ', m' when the system is in states p and q respectively. The cross sections for a transition between levels n and n', statistically averaged over states, will then be given by

$$\sigma_{n,\,n'} = \frac{1}{n^2} \sum_{\ell,\,\ell',\,m,\,m'} \sigma(n,\ \ell,\ m \to n',\ \ell',\ m') \qquad \text{(D-2)}$$

and

$$\sigma_{n',\,n} = \frac{1}{n'^2} \sum_{\ell,\,\ell',\,m,\,m'} \sigma(n', \ell', m' \to n, \ell, m). \qquad \text{(D-3)}$$

when Eq. (D-1) is used, the last equation can be written as

$$\sigma_{n',n} = \frac{1}{n'^2} \frac{v_p^2}{v_q^2} \sum_{\ell,\ell',m,m'} \sigma(n,\ell,m \to n',\ell',m'). \qquad \text{(D-4)}$$

From Eqs. (D-2) and (D-4) we then get the desired relation

$$n^2 v_p^2 \sigma_{n,n'} = n'^2 v_q^2 \sigma_{n',n}, \qquad \text{(D-5)}$$

which is Eq. (7) of the text. Although this derivation is valid only for FBA cross sections, the result can be shown to be valid at all relative velocities.[78]

E. On the Formation of an Energetic Beam of Excited Hydrogen Atoms

Energetic, excited hydrogen atoms can be produced by electron capture by fast protons, electron detachment of fast H^-, or dissociation of fast molecular ions such as H_2^+ or H_3^+. Each of these atomic processes differs from the other, either in the energy dependence of the cross section or in the excited-state population of the resulting atom.

The least-violent process is the detachment of the loosely bound electron in H^-. No theoretical estimates are available for the population distribution over excited levels of the atoms produced by this process, but experimentally it has been found that this process is less effective for populating the excited levels than the dissociation of H_2^+.[11] The detachment cross section at 10 MeV is 7.5×10^{-18} cm^2/molecule in H_2 and 75×10^{-18} cm^2/atom in Ar.[49] This is comparable to the cross section for molecular dissociation, but many orders of magnitude larger than the electron-capture cross section at this energy.

Electron capture by protons and collisional dissociation of H_2^+ both result in a fractional population of the levels given by $N_n/N_1 \approx A/n^3$, where A is of order one.[11,45,46,79,80] At low energies the two processes have comparable cross sections, and it

is usually more convenient to use proton beams. The capture cross section decreases very rapidly at high energies, however, dropping off approximately as E^{-6} (Refs. 52 and 79). No experimental results have been reported at 10 MeV, but at 1 MeV the capture cross section is already down to 10^{-22} cm^2 in H_2.[52] The cross section for the dissociation process, on the other hand, has a weak energy dependence, dropping off approximately as $E^{-0.8}$ at high energies.[81-84] At 20 MeV the cross section for $H_2^+ \rightarrow H^+ + H^0$ is still quite large, being 1.62×10^{-18} cm^2/molecule in H_2 and 13.1×10^{-18} cm^2/atom in Ar.[85] This means that at high energies the dissociation process for producing a neutral beam is more efficient than the capture process by many orders of magnitude.

The cross section for the dissociation of H_3^+ is comparable to that of H_2^+,[84] but little is known about the resulting population of the excited H^0 levels.

If further enhancement of the excited-state population is required, simple gas targets must be replaced by more exotic ones, such as Li vapor[86] or a highly ionized discharge.[87]

F. Radiative Decay of the Excited Levels

The radiative decay of a quantum level n is determined by the radiative lifetime and the population of the various states of the level. The radiative lifetimes (electric dipole radiation) for excited states of the hydrogen atom have recently been calculated by Hiskes, Tarter, and Moody[32] and Hiskes and Tarter[88] in both spherical (field-free case) and parabolic (Stark case) coordinates. Since the population of the states was not known, we assumed that initially all states $(n, \ell, \pm m)$ in the field-free case or $(n_1, n_2, \pm m)$ in the Stark case were equally populated. The time development of the number of particles in the level n is then given by

$$\frac{N_n(t)}{N_n(t=0)} = \frac{1}{n^2} \sum_{\ell=0}^{n-1} (2\ell + 1) \exp\left[- \frac{t}{\tau(n, \ell)} \right] \quad \text{(F-1)}$$

for the field-free case and by

$$\frac{N_n(t)}{N_n(t=0)} = \frac{1}{n^2}\left\{\sum_{n_1=0}^{n-1} \exp\left[-\frac{t}{\tau(m=0,n_1)}\right] + \sum_{m=1}^{n-1} 2(n-m)\exp\left[-\frac{t}{\tau(n,m)}\right]\right\} \qquad (F\text{-}2)$$

for the Stark case.[89] Tarter has considered other initial distributions in some detail;[90] however, the statistical distribution used here seems appropriate, since it is consistent with the Lorentz ionization results (Sec. V.A.).

We evaluated the expressions (F-1) and (F-2) for n = 3 through 10 using the results of Hiskes and Tarter. The results are presented graphically in Fig. 24 for the field-free case and in Fig. 25 for the Stark case; the abscissa is given both in units of time and distance traveled by 10-MeV hydrogen atoms. These graphs show that the Stark levels decay somewhat faster than the field-free levels. The field-free radiative decay of the individual states of the level n = 7 is shown in Fig. 26. The short lifetime of the p state and the increase in lifetime with increasing ℓ is typical for all levels.

The field-free lifetimes are appropriate for levels for which the total fine-structure splitting exceeds the total Stark splitting, and the Stark lifetimes are appropriate when the Stark splitting exceeds the fine structure.[30,91] The total fine-structure splitting is given by[30]

$$\Delta W = 13.6\ \alpha^2(n-1)/n^4 \text{ electron volts}, \qquad (F\text{-}3)$$

where α is the fine-structure constant, and the total Stark splitting for weak fields is given by[30]

$$\Delta W = 3\ Fn(n-1)\ (a.u.)$$
$$\approx 16\times10^{-9}\ E(V/cm)\ n(n-1) \text{ electron volts}. \qquad (F\text{-}4)$$

Comparing these two expressions, we find that Stark lifetimes are appropriate for an electric field

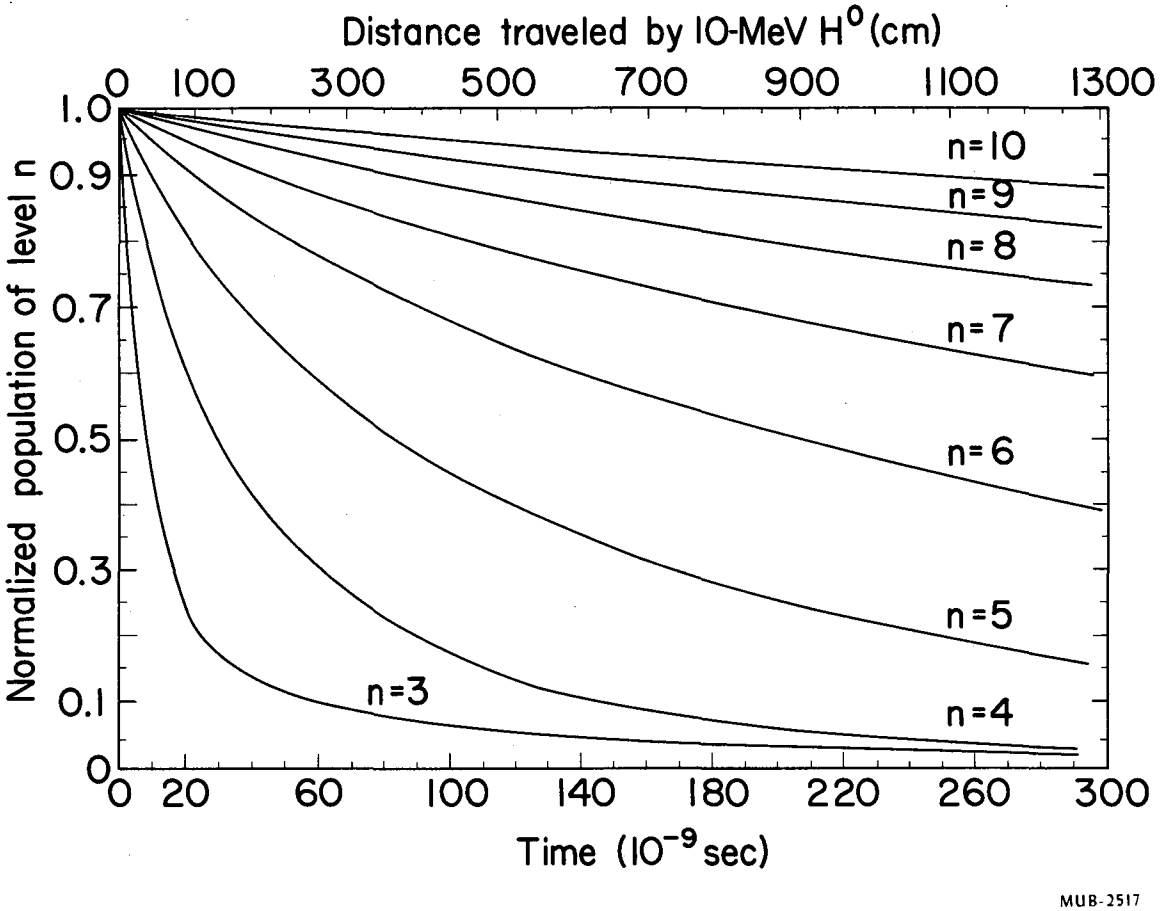

Fig. 24. Radiative decay (statistically averaged over states) of the population of the levels n = 3 to 10 for the field-free case. [Eq. (F-1)].

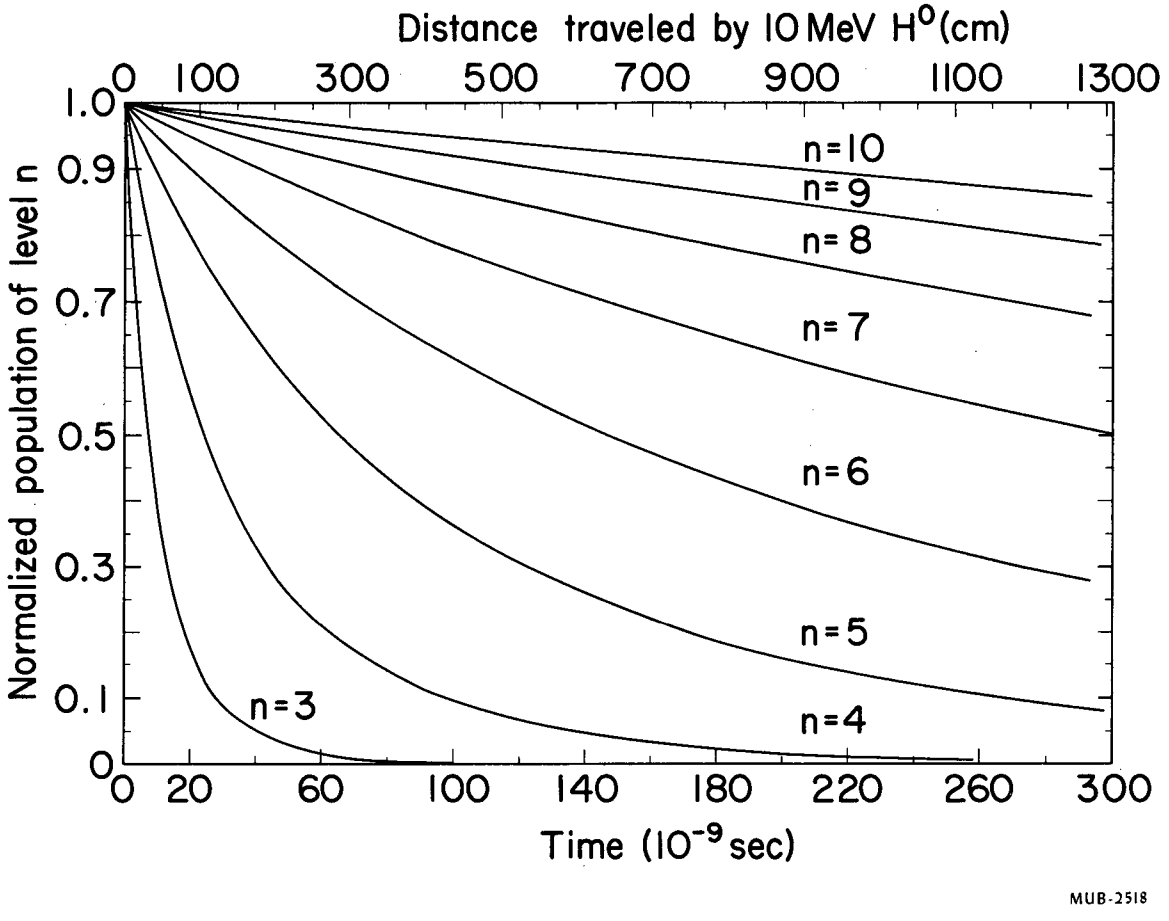

Fig. 25. Radiative decay (statistically averaged over states) of the population of the levels n = 3 to 10 for the Stark case. [Eq. (F-2)].

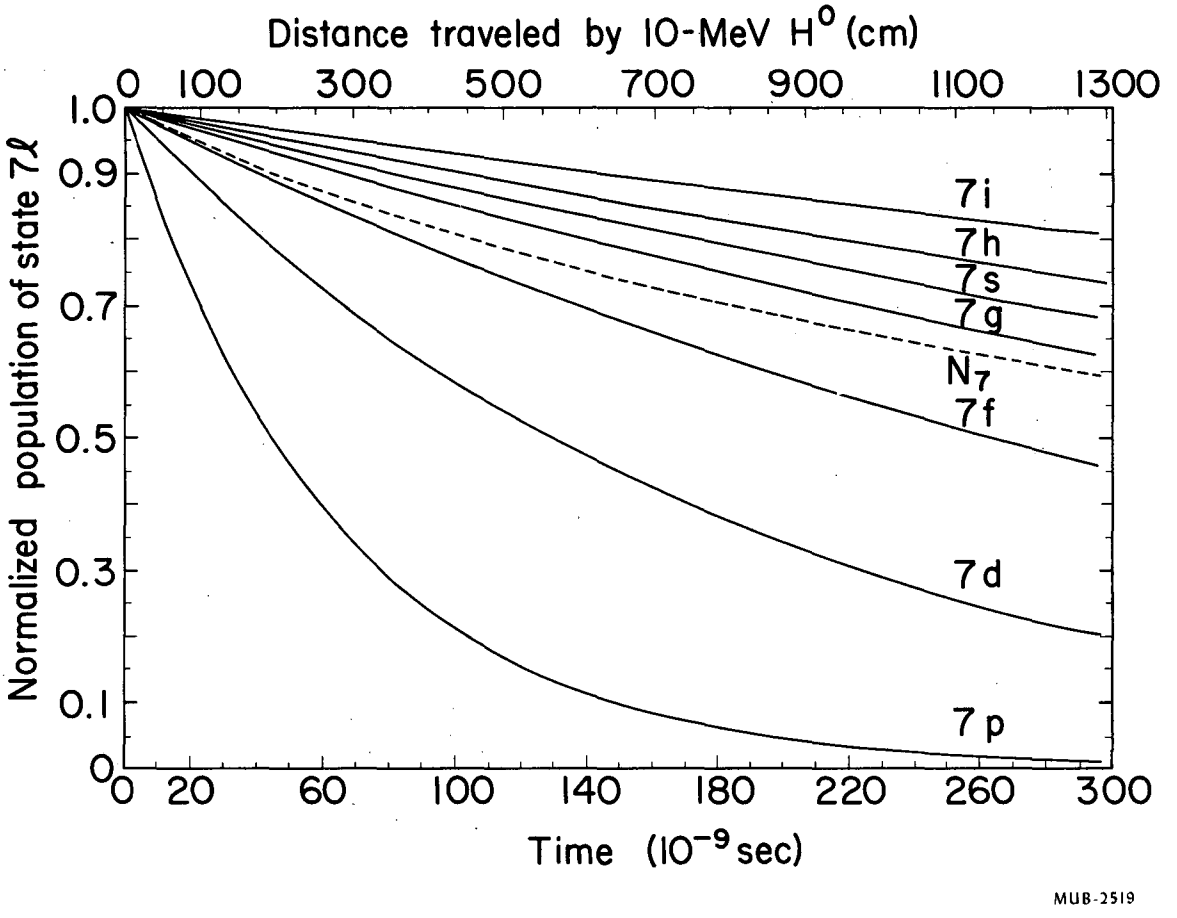

Fig. 26. Radiative decay of the population of the individual states of the level n = 7 in the field-free case. The dashed line is the statistically averaged decay rate for that level. [Eq. (F-1)].

$$F(V/cm) > \frac{4.5\times10^4}{n^5} \quad . \qquad (F\text{-}5)$$

The $\underset{\sim}{v}\times\underset{\sim}{B}$ field "seen" by a 10-MeV hydrogen atom moving through the perpendicular component of the earth's magnetic field ($\approx$ 1 gauss) is approximately 40 V/cm. In the experimental area, stray magnetic fields are present, and an average background field of 5 gauss (200 V/cm) is not unreasonable. Using Eq. (F-5), we see that Stark lifetimes are appropriate for $n \geq 5$ for the earth's field and $n \geq 3$ for the field in the experimental area. We conclude that for the levels of interest in this experiment the Stark lifetimes (Fig. 25) are appropriate.

An attempt was made to determine which of the two modes of decay was appropriate for this experiment. The neutral atoms were produced by collisional dissociation of H_2^+ in H_2 in the first and second gas cells, respectively. The populations of $n = 6$ and $n = 7$ were then compared for the two cases. Within the experimental uncertainty the results agreed with those in either Fig. 24 or Fig. 25. From these curves, the difference in the two decay modes over a 225-cm path (the distance between the exits of the two gas cells) is 5% for $n = 6$ and 2% for $n = 7$, and the present experiment does not have such precision. Longer path differences are required to determine the appropriate mode of decay for these long-lived states. Since the experimental results did not contradict the theoretical conclusions reached in the preceding paragraph, the Stark lifetimes (Fig. 25) were used in this experiment.

G. On the Use of Cross Sections for Field-Free States to Describe Transitions between Stark States

In the discussion on radiative lifetimes (Appendix F) we concluded that the $\underset{\sim}{v}\times\underset{\sim}{B}$ electric field caused by stray magnetic fields in the experimental area was sufficient to require the use of parabolic, rather than spherical, wave functions. Since theoretical collision cross sections have been published only for field-free transitions, we must consider the relationship between these two cases. In the high-energy region, the Born cross sections reduce to the Bethe cross sections, which are of the form $\sigma(n\ell \rightarrow n'\ell') = C\ E^{-1}\ \ell n\ DE$[Eq. (3)]. The coefficient C contains the dipole matrix element connecting the initial and final states. The coefficient D contains the energy difference between the initial and final states and the cutoff momentum. Considering D to be a function of n only, Hiskes[29] has transformed the cross sections of Milford and co-workers[24] from spherical to parabolic coordinates. The cross sections for transitions between particular states differ by perhaps 30%. However, averaging over states (assuming a statistical population distribution), he finds that the cross sections for transitions from n to n' are identical for the two representations by virtues of the dipole-sum rule. For the high relative velocities of this experiment, the assumption that D is a function of n only introduces an error of less than 5%, which is much less than the experimental uncertainty of the measurements. Thus a comparison of the experimental results in Stark fields with the theoretical field-free results seems justified for transitions between quantum levels n and n'.

FOOTNOTES AND REFERENCES

1. J. R. Oppenheimer, Three Notes on the Quantum Theory of Aperiodic Effects, Phys. Rev. 31, 66 (1928).
2. H. Rausch v. Traubenberg and R. Gebauer, Ueber die Erzeugung sehr hoher Elektrischer Felder zur Beobachtung des Starkeffektes, Die Naturwiss. 18, 132 (1930).
3. H. R. v. Traubenberg, R. Gebauer, and G. Lewin, Ueber die Existenzgrenzen von Anregungszustaenden des Wasserstoffatoms in Starken Elektrischen Felder, Die Naturwiss. 18, 417 (1930).
4. Cornel Lanczos, Zur Intensitaetsanomalie der Starkeffekt-Linien in sehr Starken Feldern, Die Naturwiss. 18, 329 (1930).
5. Cornel Lanczos, Zur Intensitaetschwaechung der Spektrallinien in hohen Elektrischen Feldern, Z. Physik 68, 204 (1931); 65, 431 (1930); 62, 518 (1930).
6. M. H. Rice and R. H. Good, Jr., Stark Effect in Hydrogen, J. Opt. Soc. Am. 52, 239 (1962).
7. David S. Bailey and John R. Hiskes, Ionization Rates of Hydrogen Atoms in Electric Fields, Lawrence Radiation Laboratory Report UCRL-7582, 1964.
8. D. R. Sweetman, Mirror Machine Experiments and Related Atomic Cross-Section Measurements at A. W. R. E. Aldermaston, Nucl. Fusion, 1962 Supplement, Part 1, 279 (1962).
9. A. C. Riviere and D. R. Sweetman, The Ionization of Excited Hydrogen Atoms by Strong Electric Fields, in Comptes Rendus de la VI^{e} Conference Internationale sur les Phenomenes d'Ionisation dans les Gaz (Paris, 1963), Vol. I, p. 105.
10. Selig N. Kaplan, George A. Paulikas, and Robert V. Pyle, Electron Detachment from Neutral Hydrogen by a Magnetic Field, Phys. Rev. Letters 9, 347 (1962). The steps in the experimental results of Fig. 2 are in good agreement with the calculations of Rice and Good.[6]

11. Klaus H. Berkner, John R. Hiskes, Selig N. Kaplan, George A. Paulikas, and Robert V. Pyle, The Excitation and Lorentz Ionization of 10-MeV Hydrogen Atoms, in Proceedings of the Third International Conference on the Physics of Electronic and Atomic Collisions (North-Holland Press, in press, 1963).

12. N. F. Mott and H. S. W. Massey, The Theory of Atomic Collisions (Oxford University Press, London and New York, 1949).

13. H. S. W. Massey and E. H. S. Burhop, Electronic and Ionic Impact Phenomena (Oxford University Press, London and New York, 1952).

14. M. J. Seaton, The Theory of Excitation and Ionization by Electron Impact, in Atomic and Molecular Processes, D. R. Bates, Ed. (Academic Press, New York and London, 1962), Ch. 11.

15. Wade L. Fite, The Measurement of Collisional Excitation and Ionization Cross Sections, in Atomic and Molecular Processes, D. R. Bates, Ed. (Academic Press, New York and London, 1962), Ch. 12.

16. D. R. Bates, Theoretical Treatment of Collisions Between Atomic Systems, in Atomic and Molecular Processes, D. R. Bates, Ed. (Academic Press, New York and London, 1962), Ch. 14.

17. D. W. O. Heddle and M. J. Seaton, The Excitation and Ionization of Atoms by Electron Impact, in Proceedings of the Third International Conference on the Physics of Electronic and Atomic Collisions (North-Holland Press, Amsterdam, 1963, in press).

18. S. N. Milford, Inelastic Atomic Collisions in Plasmas, Preprint No. 64-54, Aerospace Sciences Meeting, New York, N. Y., Jan. 20-22, 1964.

19. S. N. Milford, Approximate Cross Sections for Inelastic Collisions of Electrons with Atoms. I. Allowed Transitions, Astrophys. J. 131, 407 (1960).

20. J. H. Scanlon and S. N. Milford, Approximate Cross Sections for Inelastic Collisions of Electrons with Atoms. II. Forbidden Transitions, Astrophys. J. 134, 724 (1961).

21. G. C. McCoyd, S. N. Milford, and J. J. Wahl, Born Cross Sections for Inelastic Scattering of Electrons by Hydrogen Atoms. I. 3s, 3p, 3d States, Phys. Rev. 119, 149 (1960).

22. L. Fisher, S. N. Milford, and F. R. Pomilla, Born Cross Sections for Inelastic Scattering of Electrons by Hydrogen Atoms. II. 4s, 4p, 4d, 4f States, Phys. Rev. 119, 153 (1960).

23. S. N. Milford, J. J. Morrissey, and J. H. Scanlon, Born Cross Sections for Inelastic Scattering of Electrons by Hydrogen Atoms. III. 5s, 5p, 5f, 5g States, Phys. Rev. 120, 1715 (1960).

24. Gerard C. McCoyd and S. N. Milford, Born Cross Sections for Inelastic Scattering of Electrons by Hydrogen Atoms. IV. Approximate Values for Allowed Transitions up to n = 10, Phys. Rev. 130, 206 (1963).

25. D. B. Bouthilette, J. A. Healey, and S. N. Milford, Double Inelastic Collisions of Hydrogen Atoms with Excited Hydrogen Atoms in 2, 3, 4 States, in Proceedings of the Third International Conference on the Physics of Electronic and Atomic Collisions (North-Holland Press, Amsterdam, 1963, in press).

26. J. R. Hiskes, Electric and Magnetic Dissociation and Ionization of Molecular Ions and Neutral Atoms, Nucl. Fusion 2, 38 (1962).

27. John R. Hiskes and C. Bruce Tarter, Ion Density Versus Time in the Alice and Phoenix Experiments, Lawrence Radiation Laboratory Report UCRL-7033, September 1962 (unpublished).

28. John R. Hiskes, Inverted Cascades in Energetic Neutral Hydrogen Beams, Phys. Rev. Letters 10, 102 (1963); Inverted Cascades in Neutral Injection Systems, Bull. Am. Phys. Soc., Ser. II 8, 159 (1963).

29. John R. Hiskes, Cascade Processes in Energetic Neutral Hydrogen Beams, in Comptes Rendus de la VI^{e} Conference Internationale sur les Phenomenes d'Ionisation dans les Gaz (Paris, 1963), Vol. I, p. 99.

30. H. A. Bethe and E. E. Salpeter, Quantum Mechanics of One and Two Electron Atoms (Academic Press, New York, 1957), Ch. III.

31. A. C. Riviere, Notes on the Ionization of Excited Hydrogen Atoms by Strong Electric and Magnetic Fields, U. K. A. E. A. Research Group, Culham Laboratory Report CLM-M 23, June 1963 (unpublished).

32. John R. Hiskes, C. Bruce Tarter, and D. A. Moody, Stark Lifetimes for the Hydrogen Atom, Phys. Rev. 133, A424 (1964).

33. D. R. Bates, A. Fundaminsky, J. W. Leech, and H. S. W. Massey, Excitation and Ionization of Atoms by Electron Impact, Phil. Trans. Roy. Soc. London, Ser. A, 243, 93 (1950).

34. M. J. Seaton, The Impact Parameter Method for Electron Excitation of Optically Allowed Atomic Transitions, Proc. Phys. Soc. (London) 79, 1105 (1962).

35. Equation 24 of Ref. 34 was evaluated at W_i = 5425 eV with the aid of Table III (Ref. 34) for the n to n + 1 transitions for which $\Delta\ell = 1$. These results were then statistically averaged.

36. R. McCarroll, The Excitation of the Discrete Levels of Atomic Hydrogen by Fast Electrons, Proc. Phys. Soc. (London) A70, 460 (1957).

37. D. McCrea and T. V. M. McKirgan, Electron Excitation of Atomic Hydrogen in the 2p Level, Proc. Phys. Soc. (London) 75, 235 (1960).

38. T. J. M. Boyd, Electron Excitation of Atomic Hydrogen in the 2s State, Proc. Phys. Soc. (London) 72, 523 (1958).

39. A. D. Stauffer and M. R. C. McDowell, Ionization of Excited States of Hydrogen by Electron Impact, in Comptes Rendus de la VI^{e} Conference Internationale sur les Phenomenes d'Ionisation dans les Gaz (Paris, 1963), Vol. I, p. 9.

40. F. Omidvar and E. Sullivan, Electron Impact Ionization of Highly Excited Atomic Hydrogen, in Comptes Rendus de la VI^{e} Conference Internationale sur les Phenomenes d'Ionisation dans les Gaz (Paris, 1963), Vol. I, p. 15.

41. E. W. Rothe, L. L. Marino, R. H. Neynaber, and S. M. Trujillo, Electron Impact Ionization of Atomic Hydrogen and Atomic Oxygen, Phys. Rev. 125, 582 (1962).

42. S. Geltman, M. R. H. Rudge, and M. J. Seaton, Electron Impact Ionization of Atomic Hydrogen, Proc. Phys. Soc. (London) 81, 375 (1963).

43. P. Swan, The Ionization by Electrons of the Excited 2s and 2p States of Atomic Hydrogen, Proc. Phys. Soc. (London) A68, 1157 (1955).

44. F. Mandl, The Ionization by Electron Impact of Excited Hydrogen Atoms, A. E. R. E., Harwell Report AERE T/R 1006, 1952 (unpublished).

45. John R. Hiskes, Formation of Excited Hydrogen Atoms in the Collisional Dissociation of H_2 Ions, Bull. Am. Phys. Soc., Ser. II 7, 486 (1962).

46. John R. Hiskes, On the Formation of Excited Hydrogen Atoms in the Collisional Dissociation of H_2 Ions, Lawrence Radiation Laboratory Report UCRL-6960-T, June 1962 (unpublished).

47. For a discussion of Langmuir probes, see for example, David Bohm, E. H. S. Burhop and H. S. W. Massey, The Use of Probes for Plasma Exploration in Strong Magnetic Fields, in The Characteristics of Electrical Discharges in Magnetic Fields, A. Guthrie and R.K. Wakerling, Eds. (McGraw-Hill Book Company, Inc., New York, 1949), Ch. 2.

48. Charles B. Wharton, Microwave Diagnostics for High Temperature Plasmas, University of California, Radiation Laboratory Report UCRL-4836, March 1957 (unpublished).

49. Klaus H. Berkner, Selig N. Kaplan, and Robert V. Pyle, Electron Detachment from 20-MeV D^0 and D^- Ions, Bull. Am. Phys. Soc., Ser. II 8, 605 (1963); also, ~~published in Phys. Rev., 1964.~~ Rev 134, A1461 - 1464

50. D. R. Bates and G. Griffing, Inelastic Collisions Between Heavy Particles. I: Excitation and Ionization of Hydrogen Atoms in Fast Encounters with Protons and with Other Hydrogen Atoms, Proc. Phys. Soc. (London) A66, 961 (1953).

51. J. W. Hooper, D. S. Harmer, D. W. Martin, and E. W. McDaniel, Comparison of Electron and Proton Ionization Data with the Born Approximation Predictions, Phys. Rev. 125, 2000 (1962).

52. Samuel K. Allison and M. Garcia-Munoz, Electron Capture and Loss at High Energies, in Atomic and Molecular Processes, D. R. Bates, Ed. (Academic Press, New York and London, 1962), Ch. 19.

53. W. L. Fite and R. T. Brackmann, Collisions of Electrons with Hydrogen Atoms. II. Excitation of Lyman-Alpha Radiation, Phys. Rev. 112, 1151 (1958).

54. W. L. Fite, R. F. Stebbings, and R. T. Brackmann, Collisions of Electrons with Hydrogen Atoms. IV. Excitation of Lyman-Alpha Radiation Near Threshold, Phys. Rev. 116, 356 (1959).

55. William Lichten and Sheldon Schultz, Cross Sections for the Excitation of the Metastable 2s State of Atomic Hydrogen by Electron Collision, Phys. Rev. 116, 1132 (1959).

56. R. F. Stebbings, W. L. Fite, D. G. Hummer, and R. T. Brackmann, Collisions of Electrons with Hydrogen Atoms. V. Excitation of Metastable 2s Hydrogen Atoms, Phys. Rev. 119, 1939 (1960).

57. William Lichten, Angular Distribution of Lyman-α Radiation Emitted by H(2s) Atoms in Weak Electric Fields, Phys. Rev. Letters 6, 12 (1961).

58. D. G. Hummer and M. J. Seaton, Excitation of H(2s) by Electron Impact, Phys. Rev. Letters 6, 471 (1961).

59. K. Kleinpoppen, H. Krueger, and R. Ulmer, Experimental Investigation of Excitation and Polarization of Balmer-Alpha Radiation in Electron-Hydrogen Atom Collisions, in Proceedings of the Third International Conference on the Physics of Electronic and Atomic Collisions (North-Holland Press, Amsterdam, 1963, in press); also Physics Letters 2, 78 (1962).

60. H. S. W. Massey and E. H. S. Burhop, Electronic and Ionic Impact Phenomena (Oxford University Press, London and New York, 1952), p. 170-1.

61. A. J. Taylor and P. G. Burke, The Scattering of Electrons by Hydrogen Calculated by the Second Born and Close Coupling Approximation, in Proceedings of the Third International Conference on the Physics of Electronic and Atomic Collisions (North-Holland Press, Amsterdam, 1963, in press).

62. J. H. Tait and A. J. Taylor, The 1s-2s Excitation of Hydrogen Atoms by Electron Impact, Calculated with the Use of the Second Born Approximation Inclusive of Exchange, A. E. R. E. (Harwell) Theoretical Physics Division Report AERE-R 4339, May 1963 (unpublished).

63. P. D. Robinson, The Effects of Degeneracy on the Inelastic Scattering of Electrons and Protons by Hydrogen Atoms, Proc. Phys. Soc. (London) 81, 15 (1963).

64. Philip G. Burke, Harry M. Schey, and Kenneth Smith, Collisions of Slow Electrons and Positrons with Atomic Hydrogen, Phys. Rev. 129, 1258 (1963); see also references cited in this paper.

65. W. B. Somerville, Cross Sections for Electron-Hydrogen Atom Collisions in the Born Approximation to the Reactance Matrix, Proc. Phys. Soc. (London) 82, 446 (1963).

66. P. G. Burke, V. M. Burke, I. C. Percival, and R. McCarroll, Electron Scattering by Atomic Hydrogen in the 1s, 2s, or 2p State: I, Proc. Phys. Soc. (London) 80, 413 (1962).

67. V. M. Burke and R. McCarroll, Electron Scattering by Atomic Hydrogen in the 1s, 2s, or 2p State: II, Proc. Phys. Soc. (London) 80, 422 (1962).

68. R. Damburg and R. Peterkop, Excitation of Hydrogen by Electron Collision Allowing for Exchange and 1s-2s-2p Strong Coupling, Proc. Phys. Soc. (London) 80, 563 (1962).

69. W. B. Somerville, The Effect of Coupling to n = 3 States on Born 1s-2s and 1s-2p e-H Collision Cross Sections, Proc. Phys. Soc. (London) 80, 806 (1962).

70. R. Akerib and S. Borowitz, Application of the Impulse Approximation to the Scattering of Electrons by Atoms. I. Inelastic Scattering by Hydrogen Atoms, Phys. Rev. 122, 1177 (1961).

71. A. J. Taylor and P. G. Burke, Ionization of Hydrogen Atoms Using Close Coupling Wave Functions, in Proccedings of the Third International Conference on the Physics of Electronic and Atomic Collisions, London, 1963 (North-Holland Press, Amsterdam, in press).

72. K. Omidvar, Ionization of the Energy Levels of the Hydrogen-Like Atoms by Electron Impact, in Proceedings of the Third International Conference on the Physics of Electronic and Atomic Collisions, London, 1963 (North-Holland Press, Amsterdam, in press).

73. J. Carew and S. N. Milford, Born Cross Sections for Selected Inelastic Collisions of Protons with Hydrogen Atoms in States up to n = 10, Astrophys. J. 138, 772 (1963).

74. R. J. Bell and B. G. Skinner, Excitation of the 1s-2p Transition in Hydrogen and the 3s-3p Transition in Sodium by Nuclei, Proc. Phys. Soc. (London) 80, 404 (1962).

75. M. B. McElroy and E. S. Lovell, Effect of Resonance Charge Transfer on Excitation for Proton Hydrogen Collisions, Bull. Am. Phys. Soc. Ser. II 9, 183 (1964).

76. M. H. Mittleman, Excitation of Atomic Hydrogen by Fast Protons, Phys. Rev. 129, 190 (1963).

77. A. C. Riviere and D. R. Sweetman, Formation of Hydrogen Atoms in Excited States by Electron Capture, in Proceedings of the Third International Conference on the Physics of Electronic and Atomic Collisions, London, 1963 (North-Holland Press, Amsterdam, in press).

78. A. E. Glassgold, Introduction to Recombination in Plasmas, University of California (Berkeley), Physics Department, Atomic Collisions Research, Technical Report No. 5, Jan. 1, 1963 (unpublished).

79. J. David Jackson and Harry Schiff, Electron Capture by Protons Passing through Hydrogen, Phys. Rev. 89, 359 (1953).

80. S. V. Bobashov, E. P. Andreyev, and V. A. Ankudinov, Excitation of Balmer Series Spectral Lines of Hydrogen Upon Passage of H^+, H_2^+, and H_3^+ Ions through Helium and Neon, Zh. Eksperim. i. Teor. Fiz. 45, 1759 (1963).

81. H. Röpke und H. Spehl, Herstellung Eines Neutralen Wasserstoff-atomstrahl, Nucl. Inst. Methods 17, 169 (1962).

82. A. C. Riviere and D. R. Sweetman, A Search for Vibrational Energy Effects in the Dissociation of H_2^+ Ions by H_2 Gas, Proc. Phys. Soc. (London) 78, 1215 (1961).

83. D. R. Sweetman, The Dissociation of Fast H_2^+ Ions by Hydrogen, Proc. Roy. Soc. (London) A256, 416 (1960).

84. G. W. McClure, Charge Exchange and Dissociated of H^+, H_2^+, and H_3^+ Ions Incident on H_2 Gas, Phys. Rev. 130, 1852 (1963).

85. Robert V. Pyle, Klaus H. Berkner, Selig N. Kaplan, and J. Warren Stearns, Collisional Breakup of 20-MeV H_2^+ Ions, Bull. Am. Phys. Soc. Ser. II 9, (1964). (To be published April 1964).

86. Archer H. Futch, Jr. and Charles C. Damm, Enhancement of the Excited State Population in a Hydrogen Atom Beam, Nucl. Fusion 3, 124 (1963).

87. John S. Luce and John L. Hilton, Massive Conversion of 750 keV Ions to Neutrals of Quantum Levels > 7, in Comptes Rendus de la VI^{e} Conference Internationale sur les Phenomenes d'Ionisation dans les Gaz (Paris, 1963), Vol. I, p. 83.

88. John R. Hiskes and C. Bruce Tarter, Stark Lifetimes for the Hydrogen Atom, Lawrence Radiation Laboratory Report UCRL-7088 and UCRL-7088 (Rev. I), July 1963 (unpublished). Note that in Fig. 2 of UCRL-7088 the abscissa should be labeled m, not n_1. Also, C. B. Tarter and J. R. Hiskes, Radiative Lifetimes for the H Atom, Bull. Am. Phys. Soc. Ser. II 8, 159 (1963).

89. The weak dependence of $\tau(n_1, n_2, m)$ on n_1 and n_2 for $m > 0$ makes it permissible to use $\tau(n, m)$ for $m > 0$. See the discussion in UCRL-7088, Ref. 88.

90. C. Bruce Tarter, The Coefficients Connecting the Stark and Field-Free Wave Functions for Hydrogen: Theory and Application to Lorentz Dissociation, Lawrence Radiation Laboratory Report UCRL-7493, September 1963 (unpublished).

91. H. Lueders, Der Starkeffekt des Wasserstoffes bei kleinen Feldstaerken, Ann. Physik, Folge 6, 8, 301 (1951).